frontiers in Marine Science

ORIGINAL RESEARCH
published: 16 July 2019
doi: 10.3389/fmars.2019.00381

A New Vent Limpet in the Genus *Lepetodrilus* (Gastropoda: Lepetodrilidae) From Southern Ocean Hydrothermal Vent Fields Showing High Phenotypic Plasticity

Katrin Linse[1], Christopher Nicolai Roterman[2] and Chong Chen[3]*

[1] British Antarctic Survey, Cambridge, United Kingdom, [2] Department of Zoology, University of Oxford, Oxford, United Kingdom, [3] X-STAR, Japan Agency for Marine-Earth Science and Technology (JAMSTEC), Yokosuka, Japan

The recently discovered hydrothermal vent ecosystems in the Southern Ocean host a suite of vent-endemic species, including lepetodrilid limpets dominating in abundance. Limpets were collected from chimneys, basalts and megafauna of the East Scotia Ridge segments E2 and E9 and the Kemp Caldera at the southern end of the South Sandwich Island arc. The limpets varied in size and shell morphology between vent fields and displayed a high degree of phenotypic plasticity. Size frequency analyses between vent fields suggests continuous reproduction in the limpet and irregular colonisation events. Phylogenetic reconstructions and comparisons of mitochondrial COI gene sequences revealed a level of genetic similarity between individuals from the three vent fields consistent with them belonging to a single molecular operational taxonomic unit. Here we describe *Lepetodrilus concentricus* n. sp., and evaluate its genetic distinctness and pylogenetic position with congeners based on the same gene. Results indicate that *L. concentricus* n. sp. is a sister species to *L. atlanticus* from Atlantic vents, with the two species estimated to have diverged within the last ∼5 million years.

ZooBank Registration LSIDs: Article: urn:lsid:zoobank.org:pub:88165178-DE69-4DD3-A346-1DA5E2091967.

Lepetodrilus concentricus n. sp.: urn:lsid:zoobank.org:act:843DF6B3-5945-494E-B838-5F3661CE0FC8.

Keywords: East Scotia Ridge, deep-sea, Mollusca, morphometrics, new species, phylogenetics

OPEN ACCESS

Edited by:
Wei-Jen Chen,
National Taiwan University, Taiwan

Reviewed by:
Marjolaine Matabos,
Institut Français de Recherche pour l'Exploitation de la Mer (IFREMER), France
Junlong Zhang,
Institute of Oceanology (CAS), China

****Correspondence:***
Katrin Linse
kl@bas.ac.uk

Specialty section:
This article was submitted to Marine Evolutionary Biology, Biogeography, and Species Diversity, a section of the journal Frontiers in Marine Science

Received: *13 February 2019*
Accepted: *18 June 2019*
Published: *16 July 2019*

Citation:
Linse K, Roterman CN and Chen C (2019) A New Vent Limpet in the Genus Lepetodrilus (Gastropoda: Lepetodrilidae) From Southern Ocean Hydrothermal Vent Fields Showing High Phenotypic Plasticity. Front. Mar. Sci. 6:381. doi: 10.3389/fmars.2019.00381

INTRODUCTION

The first hydrothermal, black smoker vents were discovered in the Scotia Sea in 2009, within the Atlantic sector of the Southern Ocean and subsequently investigated by remotely operated vehicle (ROV) operations (Rogers et al., 2012). Fauna of the chemosynthetic chimney and diffuse flow habitats of the East Scotia Ridge (ESR) ridge segments E2 and E9 was dominated by the kiwaid yeti crab *Kiwa tyleri* Thatje in Thatje et al. (2015), the eolepadid barnacle *Neolepas scotiaensis* (Buckeridge et al., 2013), actinostolid anemones, the peltospirid snail

Gigantopelta chessoia Chen et al., 2015, and lepetodrilid limpets in the genus *Lepetodrilus*. Populations of *Kiwa tyleri*, *G. chessoia*, and *Lepetodrilus* limpets were genetically well connected between the ESR vent fields (Roterman et al., 2016). Distinct faunal elements known from Pacific and Atlantic vents, such as siboglinid worms, alvinocaridid shrimps and bathymodiolid mussels were absent. The ESR vent ecosystems showed a clear zonation of faunal assemblages along physico-chemical gradients from the vent fluid effluent to the non-hydrothermal periphery (Marsh et al., 2012). While the larger faunal elements, like the kiwaid crabs, peltospiroid gastropods, and the barnacles visually dominated the assemblages, the lepetodrilid limpets exhibited the highest abundance and was present within most assemblages along the gradient forming a clear zonation (Marsh et al., 2012). In 2010 white-smoker vent fields, diffuse flow areas and a whale fall were discovered in the Kemp Caldera at the southern end of the South Sandwich Island back-arc system (Amon et al., 2013). *Lepetodrilus* limpets were also dominant here on sulphur-encrusted chimneys and basalt structures, as well as being present on the whale skeleton albeit in lower densities (Amon et al., 2013).

The chemosynthetic habitat-endemic genus *Lepetodrilus* (Vetigastropoda: Lepetodrilidae) to date comprises 15 formally described species and occurs in hydrothermal vent, seep, wood-fall and whale-fall ecosystems of the Atlantic, Indian and Pacific Oceans (Johnson et al., 2008, MolluscaBase, 2019). First discovered with four species at hydrothermal vents on the Galápagos Rift and East Pacific Rise (EPR) (McLean, 1988), *Lepetodrilus* is the most abundant, widely distributed, and speciose genus of vent limpets. Specimens are often found epizoic on other vent-endemic megafauna such as the siboglinid giant tubeworm *Riftia* or bathymodioline mussels, commonly occurring in extremely high densities up to ∼400000 m^{-2} (Warén et al., 2006). In the last three decades, *Lepetodrilus* has been the target of various aspects of researches in vent animals. One of these four species, *Lepetodrilus elevatus* widely distributed along the EPR (21°N-38°S; McLean, 1988; Sadosky et al., 2002) actually contains four cryptic species that cannot be discriminated morphologically due to a large morphological plasticity (Matabos and Jollivet, 2019).

Lepetodrilus limpets are known to have flexible feeding strategies with the ability to feed by both grazing with radula and active suspension feeding with gill (Bates, 2007; Gaudron et al., 2015). Furthermore, Bates (2007) showed the presence of episymbionts on the gills in a study of the feeding ecology of *L. fucensis* in addition to grazing and suspension feeding. Gaudron et al. (2015) studied the nutritional partitioning of three *Lepetodrilus* species (*L. elevatus*, *L. ovalis*, and *L. pustulosus*) at the EPR, showing that they rely on both microbial and detrital (particulate organic matter) food sources. This wide variety in feeding ecology perhaps allow *Lepetodrilus* limpets to survive in areas of variable vent fluid flow.

A size- and sex-based habitat partition of *Lepetodrilus fucensis* was discovered with juveniles and males preferring the periphery, while females occurred in higher proportions in high fluid flow areas (Bates, 2007). Reproduction in lepetodrilids is believed to be continuous and together with free-swimming larvae with a planktonic dispersal stage, they are considered effective early colonisers (Kelly et al., 2007; Tyler et al., 2008; Kelly and Metaxas, 2010; Bayer et al., 2011; Nakamura et al., 2014). Tyler et al. (2008) inferred a planktotrophic over a lecithotrophic development based on comparably small oocyte sizes. The successful recolonisation after an eruption event at the EPR was studied in *L. tevnianus* by Bayer et al. (2011) and the discovery of mature specimens within a year after the eruption indicated fast maturity. Notably, Matabos et al. (2008) found that physico-chemical conditions of the immediate habitat had a significant effect on the population structure and repduction of *L. elevatus* at the 13°N vent field on the EPR.

In this study, we formally describe the *Lepetodrilus* limpet found in hydrothermal vent fields of the ESR segments E2 and E9, and the Kemp Caldera. As the collected limpets differed in shell size and shape between the different sites, morphological, and molecular analysis were carried out to determine if either a single, highly morphologically plastic species or multiple species inhabit the three sites.

MATERIALS AND METHODS

Sample Collection and Preservation

Lepetodrilus limpets were collected during expedition JC42 of RRS *James Cook* using ROV *Isis* at two vent sites in the ridge segments E2 and E9 of the ESR (Marsh et al., 2012; Rogers et al., 2012) and at one vent site in the Kemp Caldera of the southern South Sandwich Arc (**Figure 1** and **Table 1**). The distance between E2 and E9 was ∼440 km and between E9 and the Kemp Caldera, ∼90 km. *In situ*, limpets were observed on the surfaces of *Gigantopelta chessoia* snails, *Kiwa tyleri* yeti crabs, and *Neolepas scotiaensis* stalked barnacles as well as on active chimneys and basalt in diffuse flow areas (**Figure 2**). At all sites, on return of the ROV, the bioboxes, which contained either rocks collected by the manipulator arms or large megafauna specimens collected by suction sampler, and the collection barrels of the suction sampler, were emptied into sorting trays and their content visually checked and sorted into taxon specific trays. Larger macro- and megafauna as well as rocks were checked for attached fauna including *Lepetodrilus* limpets, and the latter removed. The remaining sediment material containing smaller macrofauna were fixed in bulk and later sorted under a stereomicroscope.

Specimens of *Lepetodrilus* for taxonomic and morphological studies were fixed in 96% pre-cooled ethanol for molecular and morphological analysis. Further specimens have been preserved in bulk with bottom sediment material in 96% ethanol.

Morphology

Morphometrics

Shell morphometric measurements were taken and sexes identified from a total of 591 individuals of *Lepetodrilus* from the three studied hydrothermal sites (141 from E2, 300 from E9, and 150 from Kemp Caldera).

For shell size and ratio comparisons between specimens across vent fields, the shell length (L), shell height (H), and shell widths (W) of individual *Lepetodrilus* limpet specimens were measured

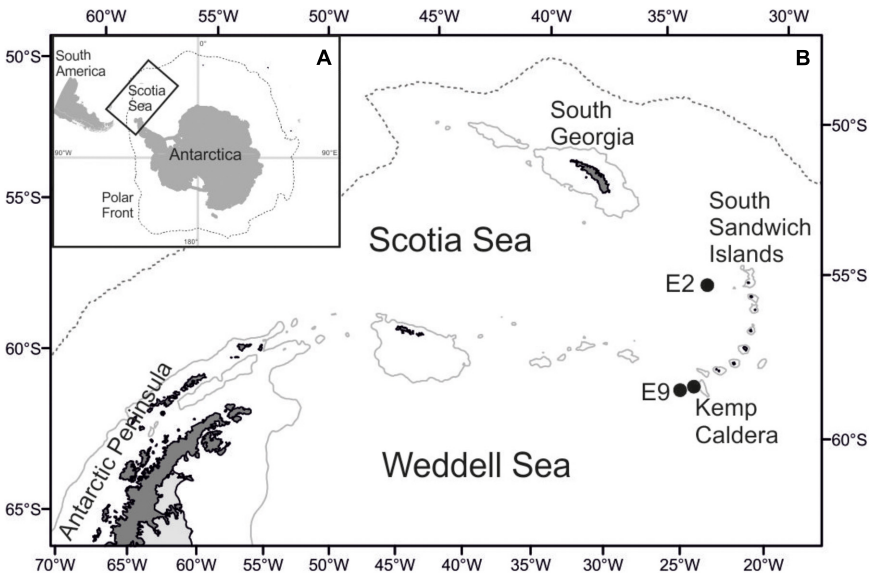

FIGURE 1 | Map of the research area. **(A)** Position of the Scotia Sea in the Southern Ocean. **(B)** Location of sampling sites at Southern Ocean hydrothermal vent fields.

TABLE 1 | Specimens measured for morphometrics.

Site	Dive	Date	Depth	Latitude	Longitude	*N*	Substrate	Museum catalogue no.
E2, ESR	*ISIS*			S	W			
Dog's Head	130	20.01.2010	2606	56°05.306	030°19.098	21	Chimney	NHMUK 20190613
Dog's Head	132	22.01.2010	2611	56°05.298	030°19.066	1	Chimney	NHMUK 20190614
Dog's Head	132	22.01.2010	2607	56°05.305	030°19.079	2	Chimney	NHMUK 20190615
Dog's Head	133	23.01.2010	2602	56°05.308	030°19.079	23	Chimney	MNHN-IM-2014-7049
Deep Castle	134	24.01.2010	2639	56°05.325	030°19.057	29	Chimney	MNHN-IM-2014-7050
Deep Castle	134	24.01.2010	2644	56°05.340	030°19.070	49	Chimney	UMZC 2019.29
Crab City	135	25.01.2010	2641	56°05.348	030°19.131	16	Kiwa tyleri	NHMUK 20190616
E9, ESR								
Marshland	141	30.01.2010	2394	60°02.807	029°58.708	93	*Neolepas scotiaensis*	NHMUK 20190617
Ivory Tower	142	01.02.2010	2396	60°02.823	029°58.696	57	*Neolepas scotiaensis*	MNHN-IM-2014-7051
Marshland	144	02.02.2010	2398	60°02.822	029°58.722	150	Off vent, on *Kiwa tyleri*	NHMUK 20190618
Kemp Caldera								
Whale fall	148	07.02.2010	1444	59°41.599	028°21.114	13	Off vent	NHMUK 20190619
Winter Palace	149	09.02.2010	1434	59°41.695	028°20.982	15	Sulphur chimney	UMZC 2019.27
Ash Mount	149	09.02.2010	1462	59°42.065	028°21.237	65	*Sericosura* spp.	NHMUK 20190620
Clam Road	149	09.02.2010	1486	59°42.023	028°21.230	57	Hard rock	MNHN-IM-2014-7052

N, number of individuals.

using digital Vernier callipers to 0.01 mm. Shell length was measured as the longest length from apex to anterior edge (major axis) of the shell base oval (Kelly and Metaxas, 2008), shell width as the distance between the two widest points perpendicular to the shell length axis, and height as the distance between the base oval and the tallest point of the shell when placed on a flat surface. Shell volume was calculated using the formula for an oval-based cone:

$$\text{Volume} = \frac{1}{3} \times \pi \times \frac{L}{2} \times \frac{W}{2} \times H$$

Specimens used for morphometric analysis are indicated in **Table 1**. For size-frequency analysis, shell length data were classed with the displayed number showing the maximum shell length in that class. Shell lengths were rounded up to the nearest half a mm, for examples a specimen of 7.12 shell length was assigned to the 7.50 mm size class and a specimen with 7.69 mm shell length was assigned to the 8 mm size class. Growths and size frequency patterns were analysed in Sigma Plot 13.0[1]. Statistical analyses were also carried out in the same software package

[1]http://www.sigmaplot.co.uk/

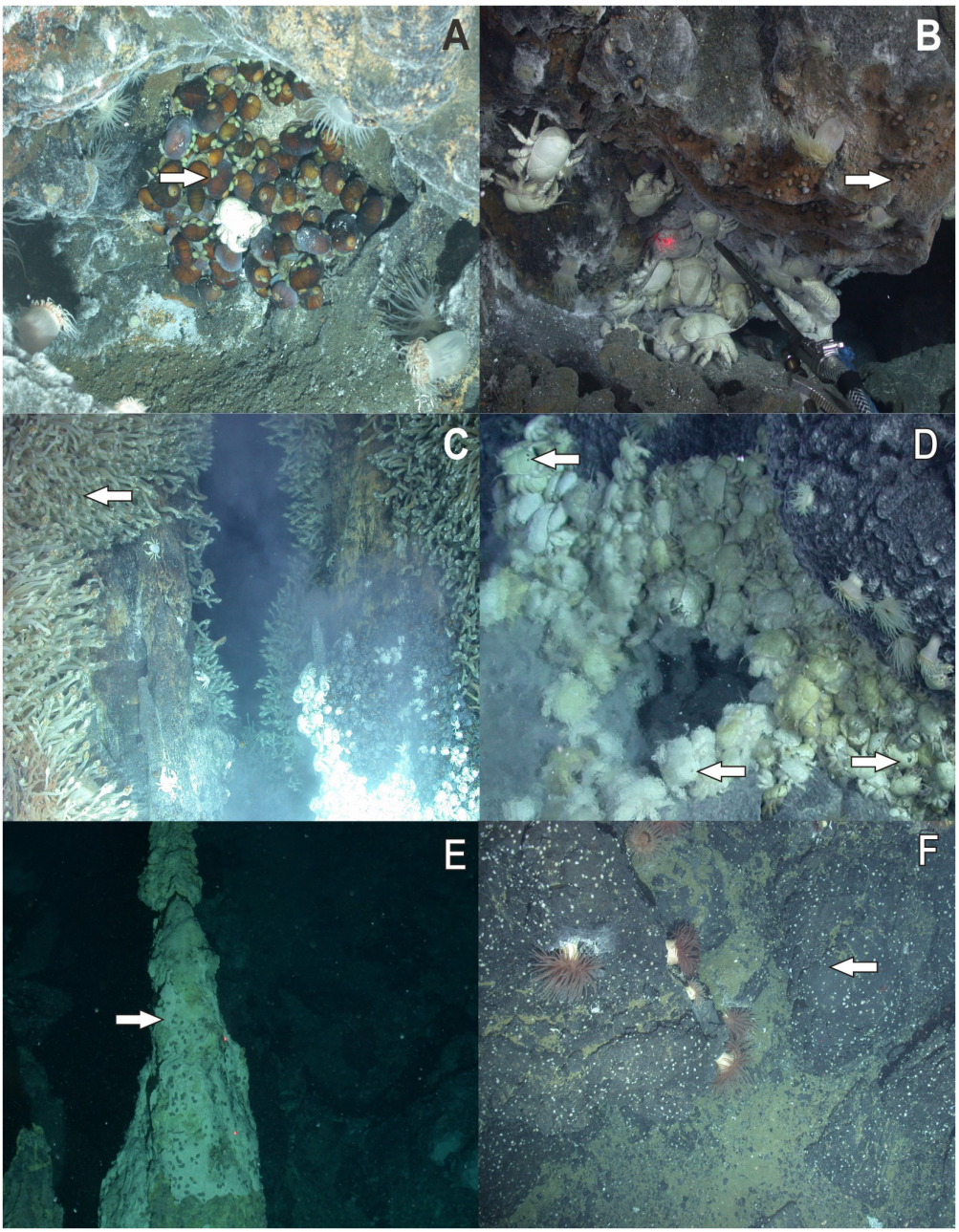

FIGURE 2 | *In situ* photographs of *Lepetodrilus concentricus* n. sp. **(A)** On *Gigantopelta chessoia* in diffuse flow near Dog's Head, E2. **(B)** On the Dog's Head chimney, E2. **(C)** On *Neolepas scotiaensis* in diffuse flow of Carwash, E9. **(D)** On *Kiwa tyleri* in diffuse flow field Marshland, E9. **(E)** On sulphur chimney in Winter Palace, Kemp Caldera. **(F)** On rocks in diffuse flow at Clam Road, Kemp Caldera. Arrows indicate position of limpets.

to examine significance of the differences observed among the three populations (E2, E9, and Kemp). The decision to use either one-way ANOVA with *post hoc* Tukey-Kramer test or the non-parametric Kruskal-Wallis test by ranks with *post hoc* Dunn's test was determined by a Shapiro-Wilk normality test.

Sex Determination

For sex determination, measured specimens were checked for the presence of a well-developed copulation appendage/penis on the right side in the neck/head area. In specimens where the foot covered the right neck area and the sex was undeterminable without damaging the specimen, the sex was recorded as unknown. Presence of a penis was observed in specimens >1.5 mm in shell length.

Scanning Electron Microscopy

Scanning electron micrographs of shells, soft parts, and radulae were made with a Hitachi TM3000 scanning electron

microscope (SEM). Radulae were prepared by dissecting the radula sac, dissolving it in 25% potassium hydroxide and cleaned for 15 s in an ultrasonic bath before SEM observation.

Genetics

DNA Sequencing

Genomic DNA was isolated from foot muscle tissue, or in the case of small specimens (<5 mm shell lengths) from the entire specimen. DNA was extracted with the DNeasy Tissue Extraction Kit (Qiagen, Crawley, West Sussex, United Kingdom) as directed by the manufacturer.

PCR amplifications were performed at the British Antarctic Survey in 40 μL volumes containing final concentrations of 1× PCR buffer (Bioline), 5% bovine serum albumin 10 mg/mL (Sigma), 200 μM each dNTP, 0.5 μM each primer (COI, ∼ 690 bp: LCO 1490 and HCO 2198 (Folmer et al., 1994) 18S, ∼ 570 bp: SSU 1F & SSU 82R (Medlin et al., 1988) 28S, ∼ 750 bp: LSU 5 and LSU 3 (Littlewood, 1994), 0.5 units of Taq DNA Polymerase (Bioline), and 1 μL template DNA. Magnesium chloride concentrations varied for each gene region: 18S, 3 mM; 28S, 3.5 mM, and COI, 2 mM.

The following cycling conditions were used: (1) COI: 94°C for 2 min followed by 35 cycles of 94°C for 30 s, 45°C for 30 s and 72°C for 45 s; (2) 18S: 94°C for 2 min followed by 35 cycles of 94°C for 1 min, 60°C for 30 s and 72°C for 1 min; and (3) 28S: 94°C for 2 min followed by 35 cycles of 94°C for 1 min, 45°C for 30 s, and 72°C for 1 min. All amplifications were finished by a final 4 min extension at 72°C. DNA sequencing was performed at LGC Berlin Germany. The following cycling conditions were used: 94°C for 2 min followed by 35 cycles of 94°C for 30 s, 45°C for 30 s, and 72°C for 45 s. All amplifications were finished by a final 4 min extension at 72°C. DNA sequencing was performed at LGC Berlin, Germany.

Additional COI fragments were also amplified at the University of Oxford using *Lepetodrilus* specific primers, LepetESR-F 5′-TAACGATATGCGTTGACCATT-3′ and LepetESR-R 5′-ACCCGGGAAGAATCAGAATA-3′ (Roterman et al., 2016), yielding a ∼620 bp fragment. These primers were designed from a larger *Lepetodrilus* COI fragment generated by 454 pyrosequencing (Leese et al., 2012). PCR Reactions were performed in 12 μl volumes, containing 0.8 μl of each primer (forward and reverse) at a concentration of 4 pmol/μl, 8 μl of Qiagen Taq Master Mix, 2 μl of DNA template (∼10–50 ng/μl) and 0.4 μl of double-distilled water. All PCR reactions were performed on a Bio-Rad C1000 Thermal Cycler. General amplification conditions were initial HotStarTaq denaturation at 95°C for 15 min, followed by 35 cycles of 94°C for 1 min, 50°C for 90 s, 72°C for 1 min, and a final extension of 72°C for 10 min.

The PCR products were visualised on 1% agarose gel using ethidium bromide. PCR products were then purified using the QIAquick gel purification kits (Cat.28106). Sequencing reactions were performed in 10 μl volumes, containing 2.5 μl cleaned PCR product, 2 μl H_2O, 2.5 μl of 0.8 pmol/μl primer, 2.5 μl BetterBuffer (or 6X Buffer), and 0.5 μl BigDyeTM. The following sequencing reaction protocol was used: initial denaturation at 96°C for 1 min, followed by 25 cycles of 96°C for 10 s, 50°C for 5 s, 60°C for 4 min, and a final cool down to 4°C. Sequences were resolved using an Applied Biosystems 3100 DNA at Department of Zoology, the University of Oxford.

Data Analyses

Consensus sequences were generated from forward and reverse strands using Geneious Pro 5.4.6 (Drummond et al., 2010), sequences were deposited in GenBank (Accession numbers KP757039-KP757103).

For phylogenetic analyses: A 633 bp alignment featuring a representative from each of the three collection sites (E2, E9, and Kemp Caldera) as well as representative COI sequences from all species/morphotypes of *Lepetodrilus* on GenBank (**Table 2**) was generated using the Geneious alignment tool in the software package Geneious Pro 5.4.6. To root the tree, we used *Pseudorimula* sp. SBJ-2008 and *Pseudorimula* sp. Lau (Johnson et al., 2008), two other species within the same family Lepetodrilidae but a different genus from *Lepetodrilus*, as the appropriate outgroup. Three different methods for determining COI phylogenies were performed in this study: maximum parsimony (MP), maximum likelihood (ML), and Bayesian inference (BI). The MP analysis was performed with PHYLIP 3.67 (Felsenstein, 2002) with 1000 bootstrap replicates. ML and BI analyses involved partitioned datasets determined using PartitionFinder 2.1 (Lanfear et al., 2016). The best partition and model scheme determined with the "all algorithm" (Guindon et al., 2010) and the Bayesian Information Criterion (BIC) was three codon partitions with the models SYM+I+G, F81+I and GTR+I+G for the 1st, 2nd, and 3rd codon partitions, respectively. The ML analysis was performed using IQ-tree 1.5.2 (Nguyen et al., 2015) with 1000 bootstrap pseudo-replicates to determine node support. BI was performed using MrBayes 3.2.6 (Ronquist and Huelsenbeck, 2003). Metropolis coupled Monte Carlo Markov Chains (MCMC) were run for 10 million generations in two simultaneous runs, each with four differently heated chains. Convergence of the analyses was validated by the standard deviation of split frequencies and examination of the potential scale reduction factors (PSRFs) in MrBayes and by monitoring of the likelihood values over time using Tracer v1.7 (Rambaut et al., 2018). Topologies were sampled every 1000 generations and the first 2500 trees (25%) were discarded as "burn in." Output consensus trees were visualised in FigTree 1.4.3.

Automatic barcode gap discovery (ABGD) analysis (Puillandre et al., 2012) was performed on a 633 bp alignment of all non-identical ESR and Kemp Caldera *Lepetodrilus* sp. sequences from this study to corroborate phylogenetic and morphological hypotheses regarding species delineation. In addition to sequences generated herein, lepetodrilid sequences reported from Johnson et al. (2006, 2008), and Nakamura et al. (2014) as well as unpublished sequences submitted in 2008 and 2013 by Shannon Johnson (GenbBank accession numbers DQ228006-DQ228070, EU306388-EU306484, AB820805-AB820839, EU306485-EU306517, and JN978011- JN978110, respectively) were also included, totalling 341 sequences. Matabos and Jollivet (2019) revisited the *L. elevatus* species complex and included most sequences of *Lepetodrilus* aff. *galriftensis* from Johnson et al. (2008) in their *L. elevatus* Clade 2 but the sequence (GenBank accession number EU306413) we used for *Lepetodrilus* aff. *galriftensis* was not included. ABGD

TABLE 2 | Details of mitochondrial COI gene sequences used in the genetic analyses.

Species	GenBank Acc. #	Sampling location	References
Pseudorimula sp. Lau	AB365216	Lau Basin	Kano, 2008
Pseudorimula sp. SBJ 2008	EU306388	North Fiji Basin	Johnson et al., 2008
Lepetodrilus fucensis	DQ228006	Explorer/Juan de Fuca ridges	Johnson et al., 2006
Lepetodrilus gordensis	DQ228028	Gorda/Nesca Ridges	Johnson et al., 2006
Lepetodrilus tevnianus	EU306389	North East Pacific Ridge	Johnson et al., 2008
Lepetodrilus aff. *tevnianus*	EU306395	East Pacific Rise	Johnson et al., 2008
Lepetodrilus elevatus	EU306405	North East Pacific Ridge	Johnson et al., 2008
Lepetodrilus aff. *elevatus*	EU306412	East Pacific Rise	Johnson et al., 2008
Lepetodrilus aff. *galriftensis*	EU306413	East Pacific Rise	Johnson et al., 2008
Lepetodrilus sp. SBJ 2009	EU306419	Costa Rica Margin	Johnson et al., 2008
Lepetodrilus cristatus	EU306428	East Pacific Rise	Johnson et al., 2008
Lepetodrilus aff. *schrolli*	EU306431	Mariana Trough	Johnson et al., 2008
Lepetodrilus schrolli	EU306437	Manus Basin	Johnson et al., 2008
Lepetodrilus nux	EU306443	Okinawa Trough	Johnson et al., 2008
Lepetodrilus pustulosus	EU306457	East Pacific Rise	Johnson et al., 2008
Lepetodrilus aff. *pustulosus*	EU306465	East Pacific Rise	Johnson et al., 2008
Lepetodrilus ovalis	EU306484	Monterey Bay/East Pacific Rise	Johnson et al., 2008
Lepetodrilus sp. 1 SBJ 2008	EU306477	Central Indian Ridge	Johnson et al., 2008
Lepetodrilus sp. 2 SBJ 2008	EU306471	Central Indian Ridge	Johnson et al., 2008
Lepetodrilus atlanticus A3117.2	EU306446	Mid Atlantic Ridge	Johnson et al., 2008
Lepetodrilus atlanticus A3117.4	EU306447	Mid Atlantic Ridge	Johnson et al., 2008
Lepetodrilus atlanticus A3117.5	EU306448	Mid Atlantic Ridge	Johnson et al., 2008
Lepetodrilus atlanticus GV.1	EU306449	Mid Atlantic Ridge	Johnson et al., 2008
Lepetodrilus atlanticus GV.2	EU306450	Mid Atlantic Ridge	Johnson et al., 2008
***Lepetodrilus concentricus* n. sp. F223.1**	**KP757102**	**E2, East Scotia Ridge**	**This study**
***Lepetodrilus concentricus* n. sp. F223.3**	**KP757086**	**E2, East Scotia Ridge**	**This study**
***Lepetodrilus concentricus* n. sp. F461L.1**	**KP757103**	**E9, East Scotia Ridge**	**This study**
***Lepetodrilus concentricus* n. sp. F461L.2**	**KP757099**	**E9, East Scotia Ridge**	**This study**
***Lepetodrilus concentricus* n. sp. F461L.3**	**KP757100**	**E9, East Scotia Ridge**	**This study**
***Lepetodrilus concentricus* n. sp. F606.2**	**KP757089**	**Kemp Caldera, Scotia Sea**	**This study**
***Lepetodrilus concentricus* n. sp. F606.3**	**KP757090**	**Kemp Caldera, Scotia Sea**	**This study**
***Lepetodrilus concentricus* n. sp. F606.4**	**KP757091**	**Kemp Caldera, Scotia Sea**	**This study**
***Lepetodrilus concentricus* n. sp. F636.1**	**KP757092**	**Kemp Caldera, Scotia Sea**	**This study**
***Lepetodrilus concentricus* n. sp. F655.1**	**KP757101**	**Kemp Caldera, Scotia Sea**	**This study**
***Lepetodrilus concentricus* n. sp. F655.2**	**KP757095**	**Kemp Caldera, Scotia Sea**	**This study**
***Lepetodrilus concentricus* n. sp. F655.3**	**KP757096**	**Kemp Caldera, Scotia Sea**	**This study**
***Lepetodrilus concentricus* n. sp. F655.4**	**KP757097**	**Kemp Caldera, Scotia Sea**	**This study**

Sequences of Lepetodrilus concentricus generated in this study are highlighted in bold.

estimates the number of species without the need of *a priori* species hypotheses by identifying gaps in the distribution of pairwise distances between each sequence based on a range of priori maximum intraspecific P-distance thresholds (Pmax). A more refined set of parameters than the default set were employed on the web version of ABGD, with the same range of Pmax, but a narrower gap width to detect smaller barcoding gaps and a greater number of steps and bins for better resolution (Pmin = 0.001, Pmax = 0.100, Steps = 40, X = 1.0, Nb bins = 50) in three separate runs with Jukes-Cantor, Kimura-2-parameter, and uncorrected P-distances. To visualise the relationships between the COI haplotypes of the ESR and Kemp Caldera *Lepetodrilus* limpets and those of the most closely related taxon determined from phylogenetic analyses (*L. atlanticus*), a COI Median Joining haplotype network (Bandelt et al., 1999) was constructed in PopART[2] from a 540 bp alignment (after removal of missing data).

Bayesian estimation of divergence times were performed with BEAST 1.10.4 (Suchard et al., 2018). The same partition scheme and substitution models used in the phylogenetic analyses were employed, with substitution and clock models unlinked across all partitions and a Yule speciation model with a relaxed lognormal clock. Two independent runs were performed for 50 million generations and sampled every 1000 generations with 10% of samples removed as burn-in. Runs were combined using LogCombiner 1.10.4. BEAST output was visualised on Tracer 1.7. In addition to the BEAST analysis, the ML -based RelTime-ML function (Tamura et al., 2012) in

[2]http://popart.otago.ac.nz

MEGA7 (Kumar et al., 2016) was used, which does not require assumptions for lineage rate variations. The tree topology generated from the MrBayes phylogenetic analysis was used as the input in the RelTime analysis, with the same calibration scheme as in BEAST, detailed below.

In the absence of fossils with which to calibrate the divergence estimates, inferred vicariant events have been chosen, whereby sister or cryptic species of *Lepetodrilus* either side of a geographical feature are assumed to have diverged from a single species as a consequence of the barrier's appearance. As a gene locus commonly used for barcoding in Mollusca (e.g., Layton et al., 2014) COI is useful for resolving intra- and inter-species differences, but owing to third codon position saturation in rapidly evolving genes such as this, its utility in resolving deeper branch nodes and their ages in phylogenetic trees is highly limited (Ho et al., 2011). The use of ancient vicariant events as calibrations will result in an underestimation of true substitution rates between closely related and likely recently divergent taxa. Consequently, we have chosen to calibrate our divergence analyses with vicariant events that are as recent as possible:

(1) The formation of the Easter Microplate on the Southern East Pacific Rise ∼5.25–2.5 Ma (Naar and Hey, 1991; Rusby and Searle, 1995), which appears to have separated cryptic species within each of the *L. pustulosus* and *L. tevnianus* complexes, separating *L. pustolusus* from *L.* aff. *pustulosus,* and *L. tevnianus* from *L.* aff. *tevnianus* (*sensu* Johnson et al., 2008); (2) the formation of the Blanco Fracture Zone (BFZ) when the Blanco Transform Fault that separates the Gorda and Juan de Fuca ridges extended substantially, leading to the divergence of *L. gordensis* and *L. fucensis*. According to Hey and Wilson (1982) and Wilson et al. (1984) the BFZ opened up by ∼5 Ma after a change in rotation pole beginning ∼8.5 Ma that altered the orientation of the Blanco Transform Fault and lead to its extension. The last significant lengthening of the fault was as recently as 1.4 Ma, when 115 km was added. We therefore conservatively consider it plausible for divergence between the *L. gordensis* and *L. fucensis* lineages to have occurred sometime between ∼8.5 and 1.4 Ma.

In the RelTime analysis, the maximum and minimum age bounds for each calibrated node are as follows: (1) 5.25 and 2.5 Ma for the divergence of the *L. tevnianus* and *L. pustulosus* complexes (2) 8.5 and 1.4 Ma for the divergence of *L. gordensis* and *L. fucensis*. In the BEAST analysis, normal prior distributions were chosen for the calibrations, whereby "soft" lower and upper bounds (2.5 and 97.5%) of the prior distributions were set to the same age bounds as in the RelTime analysis (with means of 3.875 and 4.95 Ma for the Easter Microplate and BFZ, respectively). This allows for earlier and later dates to be explored by the analysis, as per the recommendations of Ho and Phillips (2009).

Type Repositories

Specimens used in the present study, including type specimens, are deposited in the Natural History Museum, London (NHMUK), the Cambridge Zoology Museum, Cambridge, United Kingdom (UMZC), and the Muséum National d'Histoire Naturelle (MNHN), Paris, France (**Table 1**).

RESULTS

Systematics

Subclass Vetigastropoda Salvini-Plawen, 1980.
Superfamily Lepetodriloidea McLean, 1988.
Family Lepetodrilidae McLean, 1988.
***Lepetodrilus* McLean, 1988.**
Type species: *Lepetodrilus pustulosus* McLean, 1988 (by original designation).

Lepetodrilus concentricus n. sp.

(Figures 3, 4)

Lepetodrilus n. sp. 1 – Rogers et al., 2012: 6, 11, 14, 15, Figure 3, S2 and Table 2, S3, S6; Rogers and Linse, 2014: 242, Table 1.
Lepetodrilus n. sp. – Marsh et al., 2012: 6, 7, 8, Figures 5, 6 and Table 1; Roterman et al., 2013a: Table 1.
Lepetodrilus sp. nov. – Leese et al., 2012: 5, 6, 7, 12, 17, 18, Figure 7 and Tables 1–7.
Lepetodrilus nov. sp. – Rogers and Linse, 2014: 243.
Lepetodrilus sp. – Roterman et al., 2013a: 835, 839; Amon et al., 2013: 87, 91, 92, Figure 3 and Table 1; Buckeridge et al., 2013: 552, Figure 11; Reid et al., 2013: 3, 4, 8, 9, 10, Tables 3, 4; Rogers and Linse, 2014: 242, 243, Figure 3; Roterman et al., 2016: 1073, 1074, 1076, 1077, 1078, 1079, 1083, and 1084, Figures 2–4, Tables 1–4.

ZooBank Registration

urn:lsid:zoobank.org:act:843DF6B3-5945-494E-B838-5F3661CE0FC8.

Diagnosis

A medium-sized *Lepetodrilus* with rather regular, distinct, and concentric ribs. Thick brown to brown-green periostracum covering the thin shell, with concentric ribs from the shell clearly seen also on the periostracum. The position of the apex located at the posterior end of the shell aperture.

Type Material

Holotype, **Figure 3A** (NHMUK 20190608), Dog's Head, E2 vent field, ESR, 56°05.306′S 30°19.098′W, 2606 m depth, ROV *Isis* dive 130, RSS *James Cook* cruise JC42, coll. 20.01.2010, leg. Katrin Linse.

Paratype 1, **Figure 3B** (MNHN-IM-2014-7040), Crab City, E2 vent field, ESR, 56°05.348′S 030°19.131′W, 264 m depth, ROV *Isis* dive 135, RSS *James Cook* cruise JC42, coll. 25.01.2010, leg. Katrin Linse.

Paratype 2, **Figure 3C** (NHMUK 20190609), Clam Road, Kemp Caldera, 59°42.023′S 028°21.230′W, 1486 m depth, ROV *Isis* dive 149, RSS *James Cook* cruise JC42, coll. 09.02.2010, leg. Katrin Linse.

Paratype 3, **Figure 3D** (MNHN-IM-2014-7041), Winter Palace, Kemp Caldera, 59°41.695′S 028°20.982′W, 1434 m depth, ROV *Isis* dive 149, RSS *James Cook* cruise JC42, coll. 09.02.2010, Leg. Katrin Linse.

Paratype 4, **Figure 4A** (NHMUK 20190610), SEM stubs for shell, Ivory Tower, E9 vent field, ESR, 60°02.823′S 029°58.696′W, 2396 m depth, ROV *Isis* dive 142, RSS *James Cook* cruise JC42, coll. 01.02.2010, Leg. Katrin Linse.

FIGURE 3 | Lateral (1), ventral (2), and dorsal (3) views on *Lepetodrilus concentricus* n. sp. **(A)** Holotype NHMUK 20190608 from E2 (Dog's Head chimney). **(B)** Paratype 1 MNHN-IM-2014-7040 from E2 (Crab City). **(C)** Paratype 2 NHMUK 20190609 from the Kemp Caldera (Clam Road). **(D)** Paratype 3 MNHN-IM-2014-7041 from the Kemp Caldera (Winter Palace sulphur chimney) Scale bars are 5 mm.

Paratype 5, **Figure 4B** (MNHN-IM-2014-7042), SEM stub for protoconch, Deep Castle, E2 vent field, ESR, 56°05.325′S 030°19.057′W, 2639 m depth, ROV Isis dive 134, RSS James Cook cruise JC42, coll. 24.01.2010, Leg. Katrin Linse.

Paratype 6, **Figures 4C,D** (NHMUK 20190611), SEM stub for external anatomy, Marshland, E9 vent field, ESR, 60°02.807′S 029°58.708′W, 2394 m depth, ROV *Isis* dive 141, RSS *James Cook* cruise JC42, coll. 30.01.2010, Leg. Katrin Linse.

Paratype 7, **Figures 4E,F** (MNHN-IM-2014-7043), dried on SEM stub for external anatomy, Deep Castle, E2 vent field, ESR, 56°05.325′S 030°19.057′W, 2639 m depth, ROV Isis dive 134, RSS James Cook cruise JC42, coll. 24.01.2010, Leg. Katrin Linse.

Paratype 8, **Figures 4G,H** (NHMUK 20190612), SEM stub for radula, Deep Castle, E2 vent field, ESR, 56°05.325′S 030°19.057′W, 2639 m depth, ROV *Isis* dive 134, RSS *James Cook* cruise JC42, coll. 24.01.2010, Leg. Katrin Linse.

Paratype 9, **Figures 4I,J** (MNHN-IM-2014-7044), SEM stub for jaws, Deep Castle, E2 vent field, ESR, 56°05.325′S 030°19.057′W, 2639 m depth, ROV Isis dive 134, RSS James Cook cruise JC42, coll. 24.01.2010, Leg. Katrin Linse.

Additional Materials Examined

A total of 591 specimens used for morphometrics (see **Table 1** for collection data and museum voucher numbers).

A total of 36 specimens used for molecular analyses (see **Table 2** for details and GenBank accession numbers).

Description

Shell (**Figures 3**, **4A**) medium-sized for genus with maximum shell length 11.6 mm, width 9.1 mm, height 4.7 mm; holotype (NHMUK 20190608) shell length 10.8 mm, width 8.1 mm, height 3.6 mm, majority of specimens 4–6 mm in length (**Figures 3**, **4**). Thin white calcareous shell with fine, distinct, low concentric,

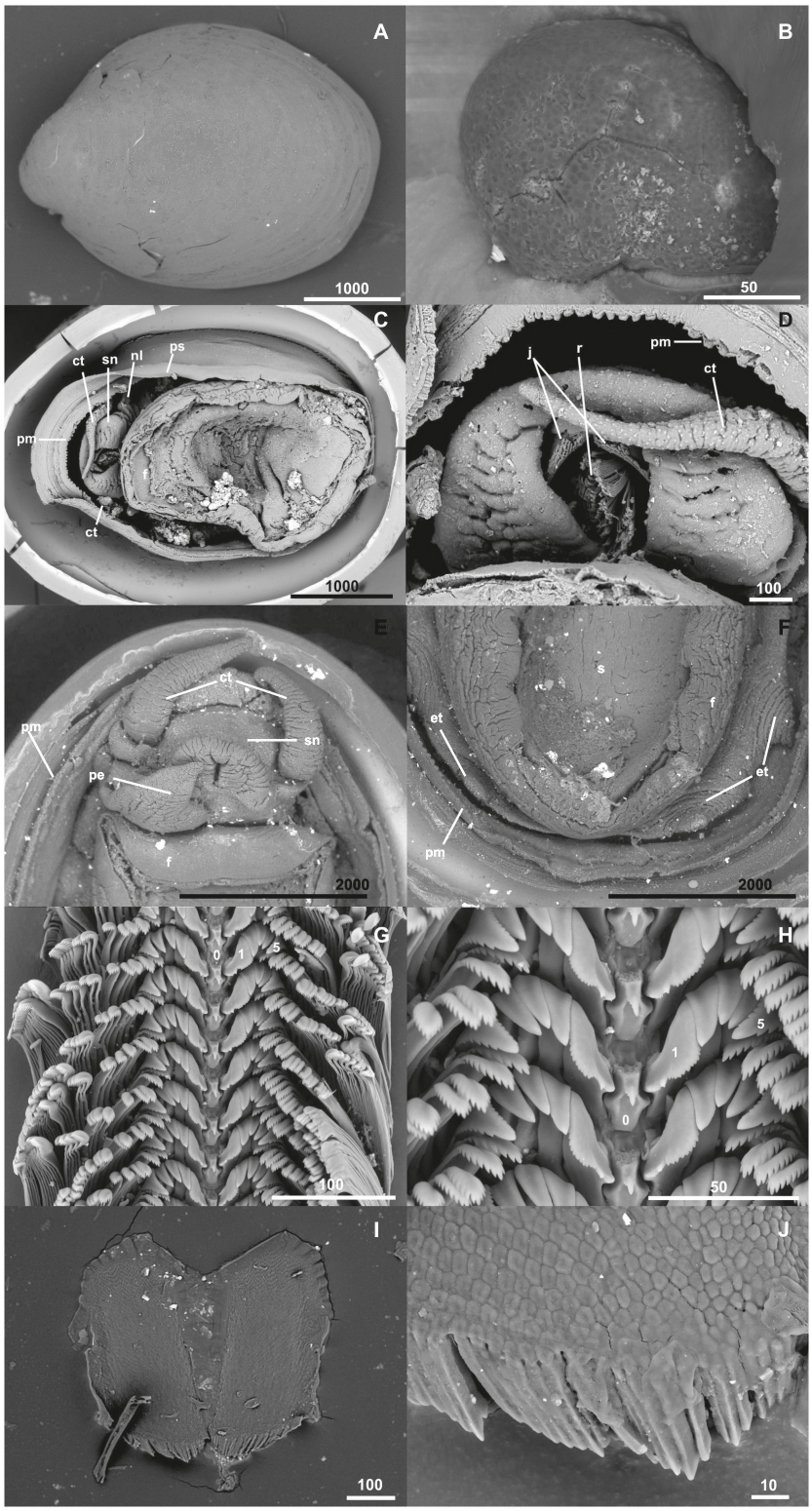

FIGURE 4 | *Lepetodrilus concentricus* n. sp., SEM micrographs. **(A)** Shell overview (Paratype 4, NHMUK 20190610), **(B)** Protoconch (Paratype 5, NHMUK 20190611), **(C)** External anatomy (Paratype 6, NHMUK 20190611), **(D)** Head and mouth with radula visible (Paratype 6, NHMUK 20190611), **(E)** penis (Paratype 7 MNHN-IM-2014-7043), **(F)** epipodial tentacles, (Paratype 7 MNHN-IM-2014-7043), **(G)** Radula overview (Paratype 8, NHMUK 20190612), **(H)** Central and lateral teeth of the radula (Paratype 8, NHMUK 20190612), **(I)** Jaws (Paratype 9, MNHN-IM-2014-7044), and **(J)** Detail of the anterior jaw margin (Paratype 9, MNHN-IM-2014-7044). ct, cephalic tentacle; f, foot; j, jaws; nl, neck lobe; ps, pallial surface (mantle edge); pm, pallial margin; r, radula; sn, snout. Scale bars in μm.

rather regular, rounded ridges; covered by thick brown green, smooth periostracum tightly adhering to shell surface and enveloping shell edge, at E2 chimneys often covered with orange or black mineral deposit layer. Apex located at posterior edge of aperture. Protoconch (**Figure 4B**) indistinctly coiled with a finely and softly pitted surface, ∼ 150 μm diameter; present in most specimens at E2 and E9, corroded in most specimens in the Kemp Caldera. Specimens between locations and microhabitats are variable in shell shape, especially varying in shell height; specimens in the Kemp Caldera higher than at E2 and E9 given the same foot size (**Figure 3**). Juveniles at Kemp Caldera found attached around legs of *Sericosura* spp. pycnogonids (Arango and Linse, 2015) developed higher shells than juveniles at E2 and E9.

External anatomy (**Figures 4C–F**) with a rounded foot. Head large, snout somewhat tapering, distinctly separated from foot by a rather long neck with well-developed neck lobe. Cephalic tentacles simple, conical, longer than snout in preserved specimens. Mouth apical-ventral, with jaws and radula visible. Sexes separate with copulation appendage present latero-ventrally on right side near base of snout, well-developed in males into a penis. Penis structure simple conical with very broad base (approx. 1 mm wide under SEM; **Figure 4E**), slightly longer than wide (just over 1 mm long under SEM; **Figure 4E**), rapidly tapering into a blunt tip. A total of four prominent epipodial tentacles present on posterior part of epipodial edge, two on each side. Epipodial tentacles typical of genus being short (0.5 mm under SEM; **Figure 4F**), simple conical in shape, rapidly tapering from broad bases (approx. 0.8 mm; **Figure 4F**). Pallial margin bilobed with inner lobe strongly crenulated, pallial surface (mantle edge) smooth. Shell muscle horseshoe shaped. Gill monopectinate, visible through thin mantle roof.

Radula (**Figures 4G,H**) in a 9.0 mm shell length male was 2.4 mm long, 0.3 mm wide with ∼ 66 rows. Formula: ca. 25–5–1–5–ca. 25. Rachidian and marginal section 62 μm width and 29 μm height per row. Rachidian tooth low with broad shaft, ending as narrowly v-shaped with one strong main and 3 small lateral cusps; posterior surface concave. Lateral teeth tightly interlocking; first lateral double as wide at base than other outer laterals and widening to top, strongly asymmetric with inner side shorter, one broad main cusp flanked by 3–5 cusps on inner and >10 cusps on outer flank. Second to forth lateral similar sized and shaped, sturdily built and curved with non-serrated apical plate. Fifth lateral broader with multi-serrated apical plate comprising broad main cusp, inner flank with 8–12 cusps, outer flank with 6–7 strong cups. Marginals: with rounded, multi-serrated apical plates, with 10–12 cusps, getting slenderer from inner to outer marginals.

Jaws (**Figures 4I,J**) paired, broad U-shaped, maximum length 364 μm, consisting of numerous rounded, irregular elements.

Etymology

"*Concentricus*" (Latin), meaning concentric. This refers to the characteristic sculpture of concentric ribs on the shell.

Type Locality

Black smoker hydrothermal vent chimneys at Dog's Head, E2 vent field, ESR, 56°05.306′S 30°19.098′W, 2606 m depth.

Distribution

Known only from hydrothermal vents on the ESR segments E2 and E9 and the southern end of South Sandwich Arc in Kemp Caldera. Bathymetric range 1434 – 2644 m.

Remarks

The rather regular, concentric, shell sculpture of *Lepetodrilus concentricus* n. sp. is highly distinctive among described *Lepetodrilus* species and distinguishes it from similar sized congeners. The position of the apex at the posterior end of the shell aperture distinguishes the species from several species, e.g., *L. ovalis*, *L. pustulosus*, *L. cristatus*. It is an average-sized species within the genus, and similar to *Lepetodrilus fucensis* McLean, 1988, *Lepetodrilus gordensis* Johnson et al., 2006, and *Lepetodrilus nux* (Okutani et al., 1993) in shell length. It is rather similar to *L. atlanticus* in shape (although more variable), but it is easily distinguished by its regular concentric sculpture. *Lepetodrilus guaymasensis* McLean, 1988 is another *Lepetodrilus* species exhibiting concentric shell sculpture, but it is not regular as in *L. concentricus* n. sp. The radula cusps on the rachidian and laterals are also characteristic in *L. concentricus* n. sp. in being even further reduced when compared with *L. elevatus* McLean, 1988 and *L. fucensis* which already has reduced cusps (Bates, 2007).

Ecological Observations

Lepetodrilus concentricus n. sp. is mainly found on hard substrata (chimneys and pillow lava), stalked barnacles (*Neolepas scotiaensis*; Buckeridge et al., 2013), and yeti crabs (*Kiwa tyleri*; Thatje et al., 2015) on and in the vicinity of hydrothermal vents and diffuse flow areas (**Figure 2**). Large densities of *L. concentricus* n. sp. were found on *N. scotiaensis* in the rising diffuse flow fluids of the chimney "Black and White" at E9 with 20000 – 56000 individuals m^{-2} (Marsh et al., 2012). Carapaces of *Kiwa tyleri* hosting *L. concentricus* n. sp. showed graze marks around the attached limpets (see images in Rogers et al., 2012) indicating that these feed on the bacterial film on the carapaces or substratum. Very small juveniles (<1 mm) were found on the legs of pycnogonids of the genus *Sericosura* in diffuse flow areas in the Kemp Caldera. *Lepetodrilus concentricus* n. sp. was also present in low abundances on the whale fall discovered in the Kemp Caldera (Amon et al., 2013). Stable isotope analysis ($\delta^{13}C$, $\delta^{15}N$, and $\delta^{34}S$) gave evidence that *L. concentricus* n. sp. feeds on chemosynthetically derived food sources (Reid et al., 2013).

Molecular Relationships

A total of 65 molecular sequences of the genes 18S, 28S and COI were obtained from 36 specimens of *Lepetodrilus concentricus* n. sp. from E2, E9, and the Kemp Caldera (GenBank accession numbers KP757039-KP757103). The 28S and 18S sequences were identical for all individuals of *Lepetodrilus* irrespective of their location (E2, E9, and Kemp Caldera). Of the 18 COI sequences generated (618–657 bp), 13 unique haplotypes were obtained. The COI sequences were used to assess taxonomy and for phylogenetic analyses. The work presented here, extends the phylogenetic analyses published

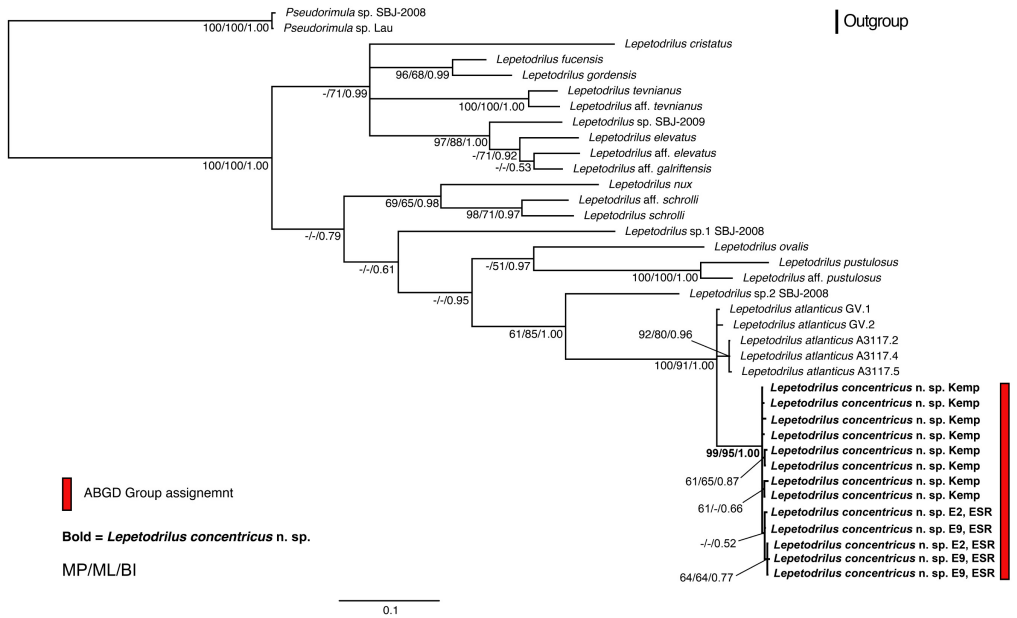

FIGURE 5 | Bayesian Inference (BI) phylogenetic tree with additional node support from maximum likelihood (ML) and maximum parsimony (MP) analyses of a 633 bp COI alignment of *Lepetodrilus*. Values adjacent to nodes are MP bootstrap pseudoreplicate percentages/ML bootstrap pseudoreplicate percentages/BI posterior probability values. The scale bar indicates BI percentage sequence divergence. ABGD refers to Automatic Barcode Gap Discovery – a method for forming species hypotheses. All nodes with $p < 0.5$ were collapsed into basal polytomies. *Lepetodrilus concentricus* n. sp. individuals are highlighted in bold.

by Rogers et al. (2012, Supplements) by substantially adding the number of lepetodrilid taxa from 13 to 20 and by extending the alignment from 522 bp to 633 bp.

With respect to COI, uncorrected pairwise distances between *Lepetodrilus* specimens recovered from vent fields on E2 and E9 and also the Kemp Caldera did not exceed 0.4%. The uncorrected pairwise distances between sequences of the most closely related taxon (see phylogenetic analyses below), L. *atlanticus*, and those from E2, E9 and the Kemp Caldera ranged from 4.2 to 5.6%. In all three ABGD runs (JC, K2P, and P) the number of defined taxonomic groups varied according to the *a priori* Pmax threshold, however, a large "barcode gap" in the P-distance distribution was evident spanning roughly 1% to 3.5–4.5%, depending on the run. With Pmax values in this range, there were 21–22 inferred taxonomic groups and in all these cases, *Lepetodrilus* individuals collected from E2, E9, and the Kemp Caldera comprised a single group. Consequently, one molecular operational taxonomic unit (MOTU) was assigned to all collected specimens corresponding to *Lepetodrilus concentricus* n. sp.

The phylogenetic relationships of *L. concentricus* n. sp. with other congeners were examined using Maximum Parsimony (MP), ML, and Bayesian Interference (BI) analyses on a 633 bp alignment of COI with other lepetodrilid species (**Figure 5**). The three types of analyses yielded different topologies with respect to deeper nodes, but were consistent with respect to the strongly supported (99 and 95% MP and ML bootstrap support, respectively, BI posterior probability of 1.00) monophyly of the *Lepetodrilus concentricus* n. sp. specimens. Within this clade, BI analyses resulted in a weak (posterior probability 0.52) support for a further clade comprising the specimens from E2 and E9, which was not supported in the MP and ML analyses. Monophyly of a larger clade comprising the *Lepetodrilus concentricus* n. sp. individuals as well as *L. atlanticus* was universally strong between the MP, ML and BI analyses (100, 91, and 1.00, respectively). The 540 bp COI median joining network (**Figure 6**) revealed a close clustering of *Lepetodrilus concentricus* n. sp. sequences; with haplotypes varying by no more than a single nucleotide from its nearest neighbour, in contrast with the relationship between *Lepetodrilus concentricus* n. sp. haplotypes and those assigned to *L. atlanticus*, which are more than 21 bp divergent. Within the *Lepetodrilus concentricus* n. sp. cluster, there appears to be a separation by region (ESR and Kemp Caldera). Bayesian calibrated divergence analysis performed in BEAST (**Figure 7A**) revealed a recent common ancestor between *L. atlanticus* and *L. concentricus* n. sp. from the Plio-Pleistocene, with a median estimate of 2.79 Ma (1.35–4.82 Ma, 95% HPD) and a median age for the common ancestor of *Lepetodrilus* at 30.68 Ma. The RelTime analysis in MEGA7 (**Figure 7B**), while producing similar ages for the tree topology as a whole, generated a younger median age for the common ancestor of *L. atlanticus,* and *L. concentricus* – 1.38 Ma (CI of 0.59–2.46 Ma) with a median age for the common ancestor of *Lepetodrilus* at 33.05 Ma.

Morphometrics and Phenotypic Plasticity

Shell length in *Lepetodrilus concentricus* n. sp. ranged from 0.7 to 11.9 mm, with the smallest specimens collected in the Kemp Caldera and the largest on the Dog's Head chimney at E2 (**Figures 8**, **9**). At ESR vents, the smallest specimens were 2.06 mm (E9) and 2.63 mm (E2). The largest specimens at E9 were 7.33 mm among those found on stalked barnacle and

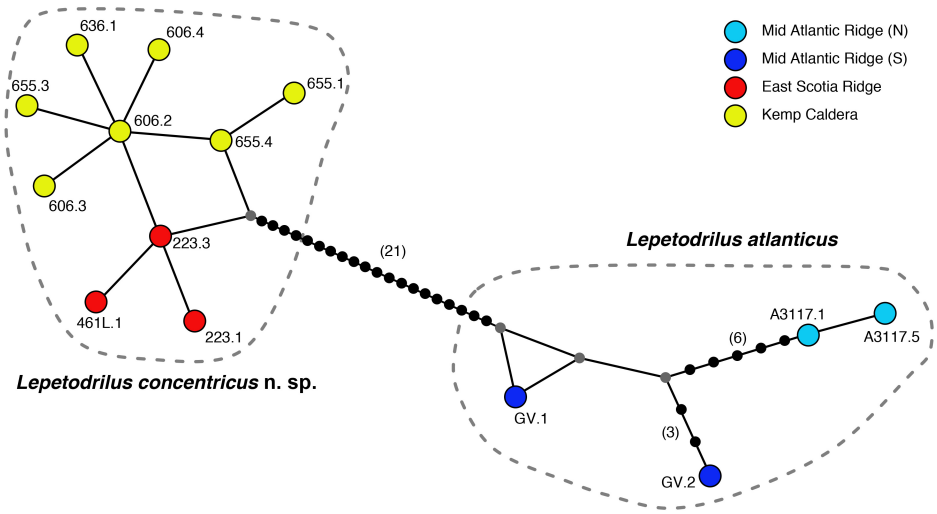

FIGURE 6 | Median-joining haplotype network using 540 bp alignment of the COI gene, showing relationships between *Lepetodrilus concentricus* n. sp. from the East Scotia Ridge and the Kemp Caldera and the closely related *L. alanticus*.

7.69 mm among those found on the basalts, and 8.18 mm in the Kemp Caldera. E9 specimens collected from *Kiwa* yeti crabs and those collected from *Neolepas* stalked barnacles did not differ in aspects of their morphometrics and were thus pooled for the analyses.

The shell measurements, the calculated shell volumes and measurement ratios were plotted against length, width, and height (**Figure 8**). Allometry was similar in all three groups, clear from visual inspection of comparisons of morphometric comparisons; plots of shell length against shell width showed a clear linear relationship (**Figure 8A**) and both independently against volume showed a clear polynomial curved relationship (**Figures 8D,E**). Plots considering the factor of shell height, either directly or in a measurement ratio, however, showed a wide variability in shell morphometrics with shells from E2 and E9 being similar to each other while shells from the Kemp Caldera differed (**Figures 8B,C**). This reflects the observation that limpets collected in the Kemp Caldera from the legs of pygnogonid *Sericosura* spp. and from habitats in the vicinity of high pygnogonid abundances showed larger shell height/width ratios than the specimens from E2 and E9 (**Figures 3**, **8C,D**); in specimens from E2 and E9 the shell height/width ratios range between 0.3 and 0.5 and did not change with increasing shell length. This observation was confirmed statistically, with shell height/width ratio being significantly different among the sites (Kruskal-Wallis test, $H = 126.497$, df = 2, $p < 0.001$) and *post hoc* Dunn's test showed that the ratio differed significantly between Kemp and both E2 ($p < 0.001$) and E9 ($p < 0.001$) while there was no difference between E2 and E9 ($p = 1.000$). Examples of the different shell morphotypes are shown in **Figure 3**, with the flat type being dominant at E2 and E9 (**Figures 3A,B**) and the raised type at the Kemp Caldera (**Figures 3C,D**).

The size frequency distributions for the specimens collected at E2, E9 and in the Kemp Caldera differed from the normal distribution (**Figure 9**). E2 was negatively skewed (**Figure 9A**) while E9 and the Kemp Caldera showed positively skewed distributions (**Figures 9B,C**). At E2 the absence of specimens <2.5 mm in length was apparent and the length frequency implied a bi-modal distribution indicating two cohorts or colonisation events. E9 and the Kemp Caldera indicated continuous colonisation or reproduction events. E9 exhibited the highest numbers of medium-sized limpets (4–5 mm in length), while at the Kemp Caldera specimens <4 mm in length were most frequent and even specimens <2 mm were common. The specimens measured at E9 and the Kemp Caldera did not reach more than 8.5 mm in length.

The sexes in the examined specimens were unequally represented and showed a subjective bias toward males, as females were defined as absence of a penis meaning the undetermined individuals (where presence of a penis was not determinable without physical damage to the specimen) could include more males. The analysis of 595 specimens revealed 318 males, 183 females, and 101 undetermined animals, which were all >6.0 mm in shell length, resulting in a male: female ratio of 1.73: 1. In general, males and females could be differentiated when shell lengths exceeded 2 mm (**Figure 9**). The largest specimens (>9 mm shell length) were all identified as males. Both sexes were represented also by small individuals of 1.5 mm in length, showing that it is already possible to sex them at this small size.

DISCUSSION

Molecular Relationships

Results of the ABGD analyses grouping all E2, E9, and Kemp Caldera limpets as one MOTU, distinct from other lepetodrilid taxa, is consistent with the lepetodrilid barcoding study of Johnson et al. (2008). The 0.4% maximum uncorrected COI p-distance within the E2, E9, and Kemp Caldera MOTU,

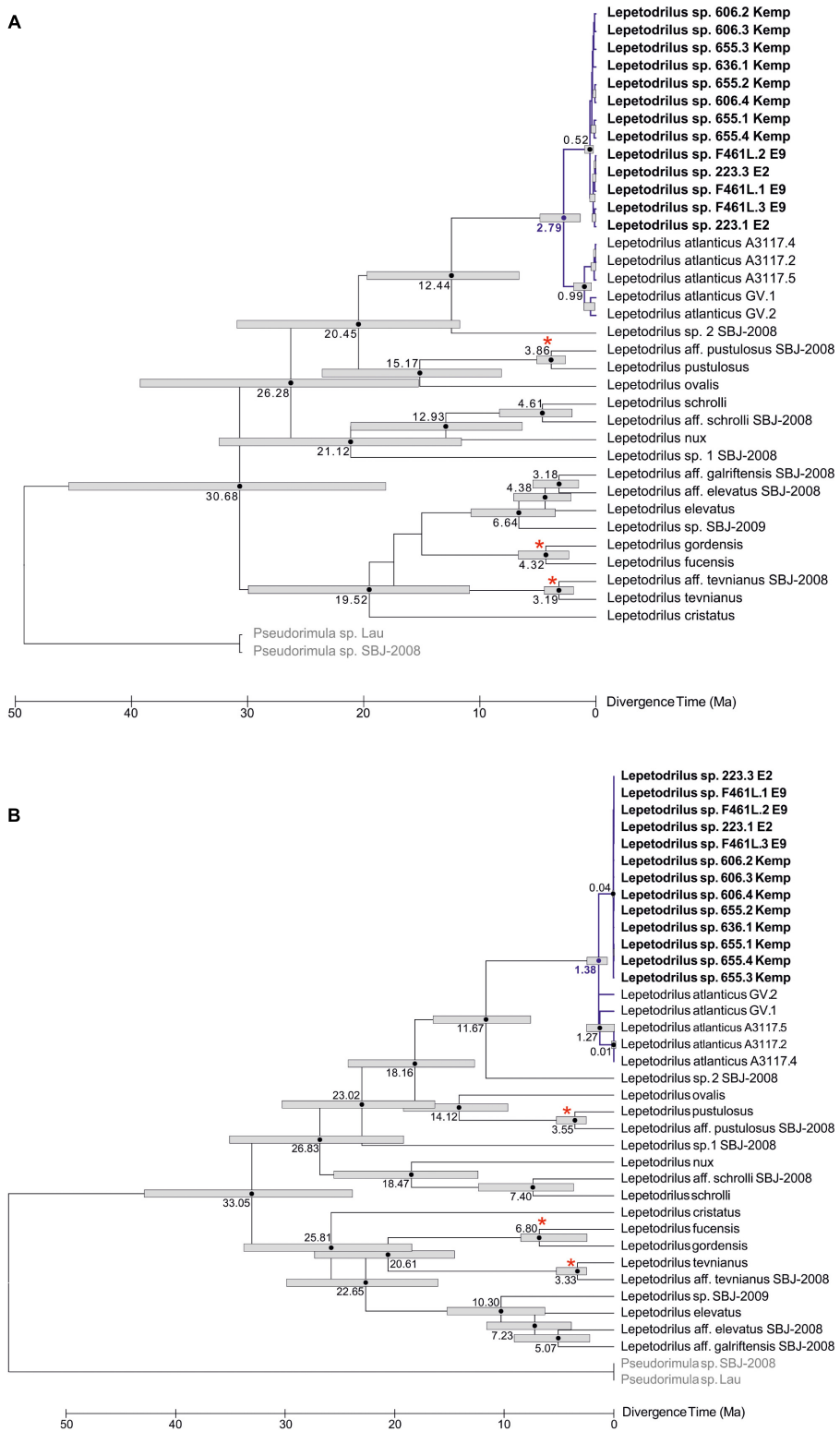

FIGURE 7 | Divergence time analyses for a 633 bp COI alignment of *Lepetodrilus*. **(A)** Bayesian divergence time estimates performed in Beast 1.10.4. Node bars represent the 95% highest posterior density (HPD) interval for nodal age. **(B)** RelTime ML divergence time estimates performed in MEGA7. Node bars represent the confidence interval for nodal age. Numbers next to node bars represent median age estimates. Nodes marked with a red asterisk are calibrated to a vicariant event. Branches and median age estimates highlighted in blue are of particular interest. *Lepetodrilus concentricus* n. sp. individuals are highlighted in bold. Outgroup species are in grey.

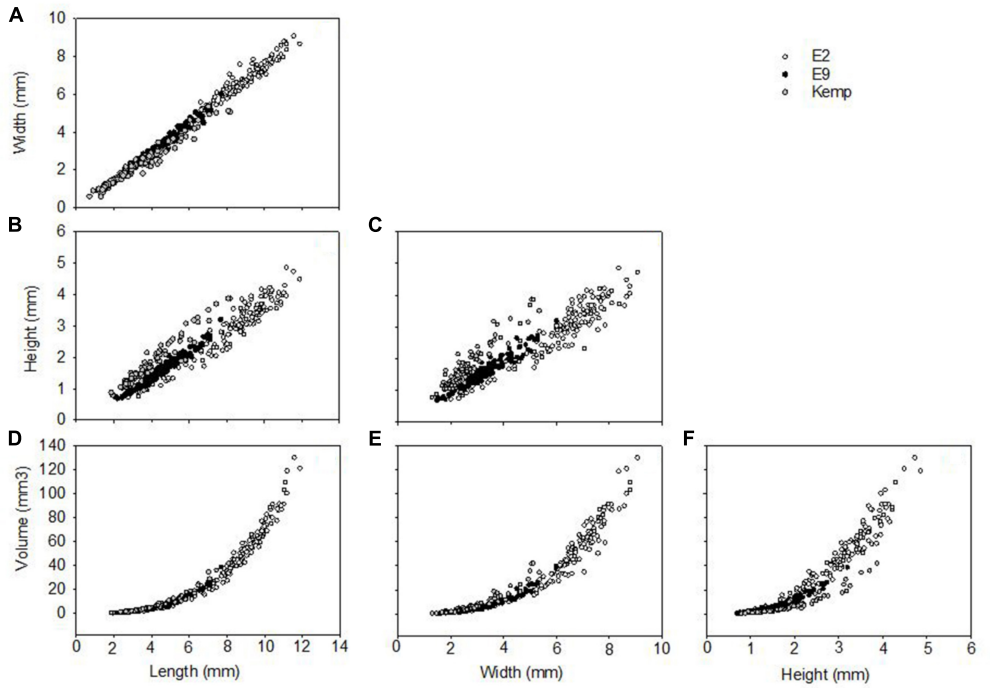

FIGURE 8 | Shell morphometrics of *Lepetodrilus concentricus* n. sp., showing relationships between **(A)** width vs. length, **(B)** height vs. length, **(C)** height vs. width, **(D)** volume vs. length, **(E)** volume vs. width, **(F)** volume vs. height. Symbols represent individual specimens measured: ○, E2; ●, E9; and ●, Kemp.

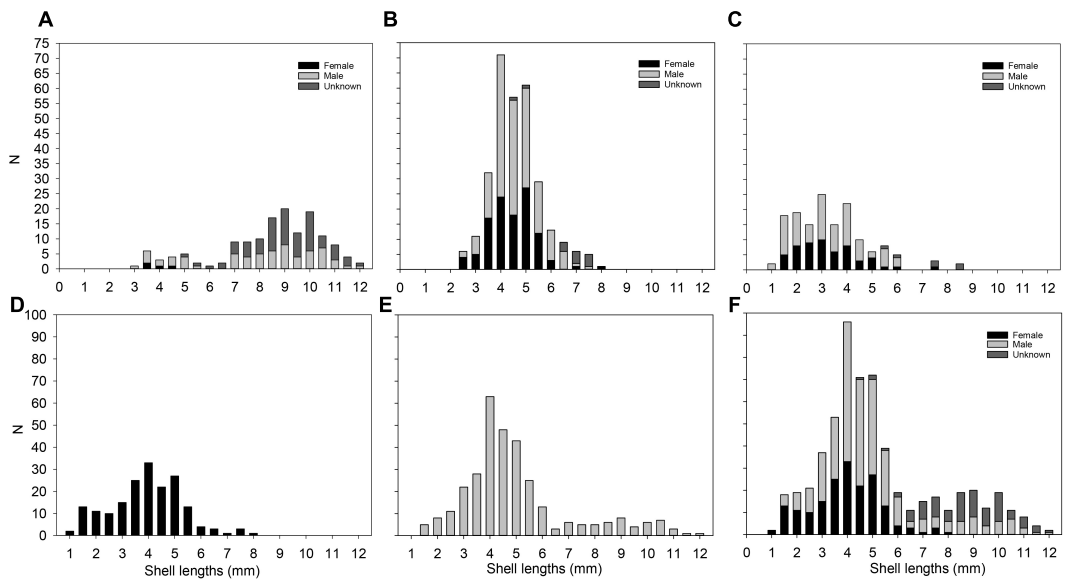

FIGURE 9 | Size-frequency distribution per site and per sex in *Lepetodrilus concentricus* n. sp. **(A)** 141 individuals from E2 in the ESR. **(B)** 300 individuals from E9 in the ESR. **(C)** 150 individuals from Kemp Caldera. **(D)** 183 females pooled from all sites. **(E)** 318 males pooled from all sites. **(F)** All 591 individuals pooled from all sites.

and the 4.2–5.6% p-distance between it and the most closely related taxon, *L. atlanticus*, fits into the 0.1–1.3% and 3.0–30.3% ranges of COI pairwise distances reported within and between MOTUs, respectively in their barcoding study. The median-joining network (but not the ABDG analyses) did reveal – despite the very low level of divergence amongst the *L. concentricus* n. sp. individuals – an apparent geographical split between limpets collected from the ESR and those from

the Kemp Caldera. A similar pattern was detected in a larger population genetics study using both COI and microsatellites on the lepetodrilids in this study and collected from the same sites (Roterman et al., 2016) where they found evidence for population structure between the ESR and Kemp (FST of ∼0.45 for COI and RST of ∼0.3 for microsatellites). The authors have speculated that the population structure, despite close proximity between the ESR and the caldera (∼95 km), may be the consequence of either physical isolation relating to the caldera's topography, the depth disparity between the two regions (∼1000 m), other hydrographic barriers or the possibility of strong selection in the presence of different physico-chemical and thermal conditions between the ESR and the Kemp Caldera (or a combination of these). Whether or not this is the case, despite very low COI pairwise differences, it remains possible therefore that some of the morphological differences between the limpets collected from the ESR and Kemp reflect evolutionary adaptive changes to the different conditions. Nevertheless, the absence of any population structure between E2 and E9 appear to rule out any genetic basis for morphological variance between *L. concentricus* n. sp. on the ESR.

In a biogeographic context, *Lepetodrilus concentricus* n. sp. belongs to one of the most common genera present at chemosynthetic ecosystems in the Atlantic, Indian, Pacific, and now the Southern oceans. The molecular analysis presented here confirms *L. atlanticus* as a sister taxon to *L. concentricus* n. sp. and could be indicative of past connectivity between vents in the Scotia Sea and those on Mid-Atlantic Ridge (MAR) via the American-Antarctic Ridge (AAR) and the Bouvet Triple Junction, a possibility considered by Tyler and Young (2003).

The divergence date analyses place the common ancestor of *L. concentricus* n. sp. and *L. atlanticus* within the last 5 million years, with median estimates in the late Pliocene and early-mid Pleistocene (2.79 and 1.38 Ma for BEAST and RelTime analyses, respectively). The analyses produced median estimates for the common ancestor of *Lepetodrilus* existing at around 31–33 Ma and no earlier than about 46 Ma, which are broadly consistent with estimates for lepetodrilid divergence reported by Vrijenhoek (2013), where it was suggested that lepetodrilids diversified in the Cenozoic after the Paleocene/Eocene Thermal Maximum, roughly 57 Ma. Whereas in some cases the divergence of closely related lepetodrilid species can be clearly attributed to the appearance of geological features disruption gene flow along a mid-ocean ridge (e.g., the Easter Microplate and cryptic speciation within the *L. pustolosus* species complex leading to the separation of *L. pustulusus* and *L.* aff. *pustulosus*), there are no obvious candidates for vicariance in the case of *L. concentricus* n. sp. and *L. atlanticus*. No substantial discontinuities are believed to have appeared along the very slow-spreading AAR within the last 5 million years (Barker and Lawver, 1988; Vérard et al., 2012). There have been some changes at the Bouvet Triple Junction – which connects the AAR to the MAR (Ligi et al., 1999) – but, none that seem likely to have impeded larval dispersal between the two ridge systems. Nevertheless, vicariance occurring along a stretch of mid-ocean ridge cannot be ruled out, given the uncertainty regarding – and limited resolution of – past ridge reconstructions. Presently the AAR connects to the South Sandwich Trench to the east of the South Sandwich Islands via the South Sandwich Fracture Zone, a large, nearly 400km long transform fault that could be a barrier for dispersing larvae between the Scotia Sea and the AAR. However, it is possible that within the last few million years spreading portions of the AAR that have since been subducted under the South Sandwich Trench (e.g., see Larter et al., 2003) could have once provided dispersal stepping stones between chemosynthetic ecosystems in the Scotia Sea and the AAR (and the MAR by extension).

In the absence of any obvious large geological changes to ridge configuration, divergence could yet have occurred through more subtle changes in ridge topography and hydrothermal activity. Changes in oceanographic conditions, e.g., water temperature or current direction and intensity could also be responsible. It may be noteworthy that the divergence dates inferred here are coincident with climatic cooling in the late Pliocene and onset of more intense glacial interglacial cycles that characterise the Pleistocene (Cortese and Gersonde, 2008). An alternative to scenarios of allopatric speciation, however, might be that the genetic distance between *L. concentricus* n. sp. and *L. atlanticus* largely reflects an isolation by distance effect (i.e., parapatric speciation). This is possibly hinted at in the median-joining network (**Figure 6**) which shows that the two *L. atlanticus* specimens collected from the Southern Hemisphere are slightly less divergent from *L. concentricus* n. sp. than those from further North. Only future sampling of intervening ridges will reveal whether or not this is the case.

The question of how *Lepetodrilus* limpets came to be in the Scotia Sea in the first place and by extension, how they came to be in the Atlantic Ocean as well, may be revealed by examining the phylogenetic tree topology. Other taxa found at vents in the Scotia Sea, including the forciplate sea star *Paulasterias tyleri*, the pygnogonids *Sericosura bamberi*, *S. curva* and *S. dimorpha*, the kiwaid squat lobster *Kiwa tyleri* and the eolepadid barnacle *N. scotiaensis* have phylogenetically basal relatives from the East Pacific, suggestive of a Pacific provenance for many of the Scotia Sea chemosynthetic taxa (Buckeridge et al., 2013; Roterman et al., 2013b, 2018; Arango and Linse, 2015; Herrera et al., 2015). Both *K. tyleri* and *N. scotiaensis*, as well as the peltospirid gastropod *G. chessoia* (Chen et al., 2015), also have closely related sister species on the Southwest Indian Ridge (SWIR). Although *Lepetodrilus* limpets have also been found on the SWIR, they have not yet been phylogenetically studied (Copley et al., 2016). Roterman et al. (2013b, 2018) and Herrera et al. (2015) have suggested that kiwaids and barnacles arrived on the ESR from Southeast Pacific ridges after the opening of Drake's Passage ∼30 Ma, via now extinct intervening ridges. These lineages subsequently spread eastward, facilitated by the Antarctic Circumpolar Current to the SWIR via the AAR, with SWIR and ESR species diverging – along with the peltospirid gastropods (Chen et al., 2015) – during the Miocene or Plio-Pleistocene. The COI divergences between the ESR and SWIR sister taxa are similar to the divergences between *L. concentricus* n. sp. and *L. atlanticus* and would be consistent with limpets spreading from the Scotia Sea eastward in a similar way to *K. tyleri* and *N. scotiaensis* and then also spreading north up the MAR at the Bouvet Triple Junction, which links the AAR, MAR, and SWIR. In this scenario, then, *Lepetodrilus* limpets would have first arrived at vents in the Scotia Sea from the

Pacific in a similar fashion to the other chemosynthetic taxa in the region. The Bayesian tree topology generated here shows a Pacific *ovalis-pustolusus* clade to be basal to a group of non-Pacific limpets comprising *L. concentricus* n. sp., *L. atlanticus* and *Lepetodrilus* sp. 2 SBJ-2008 (from the Central Indian Ridge – Johnson et al., 2008), consistent with this scenario. However, ML and MP analyses do not show sufficient (>50%) support for this topology, which is unsurprising, given the utility of COI primarily as a barcoding gene and not one for resolving deep phylogenetic relationships. Additionally, all phylogenetic analyses herein show *Lepetodrilus* sp. 2 SBJ-2008 to be basal to *L. concentricus* n. sp. and *L. atlanticus*, rather than *L. concentricus* n. sp. being basal, as would be expected if limpets spread eastward into the Southern Indian Ocean and northward into the Atlantic from the Scotia Sea.

The lack of strong support for an *ovalis-pustolusus* clade as basal to these non-Pacific limpets allows for other scenarios to be considered, such as *Lepetodrilus* limpets spreading into the Indian Ocean from the West Pacific and then subsequently into the Atlantic Ocean and Scotia Sea, for example. Past regional extinctions and subsequent radiations may also complicate attempts at reconstructing the spread of *Lepetodrilus* in the Atlantic, Indian, and Southern Oceans. Furthermore, *Lepetodrilus* has been found at a wider variety of chemosynthetic ecosystems (Johnson et al., 2008), including whale carcasses, than the other vent-associated species in the Scotia Sea. Mid-ocean ridges may therefore not necessarily be the only way in which *Lepetodrilus* has spread regionally or globally, although the divergence of *Lepetodrilus* species either side of mid-ocean ridge discontinuities in the Pacific would be consistent with largely ridge-mediated dispersal. A future multilocus phylogenetic study on *Lepetodrilus*, preferentially incorporating sequences from the species found at the SWIR (Copley et al., 2016) will be needed to shed further light on the global phylogeographic patterns of the genus.

Phenotypic Plasticity

The morphometric shell shape analyses on the three populations of *Lepetodrilus concentricus* n. sp. revealed a high phenotypic variability between specimens collected on the ESR (E2 and E9) and those from the Kemp Caldera. Given the differences in dominant attachment substrates observed between the ESR (flat surfaces of various sorts) and the Kemp Caldera (thin pycnogonid legs), a likely factor behind this is that the phenotypic variability is a response to the local substratum structure. Specimens in the Kemp Caldera were collected either from the legs of the pycnogonid *Sericosura* spp. or from habitats with high pycnogonid abundances, which had a distinct higher length/width ratio giving the shell shape a laterally flattened and raised appearance. Newly settled or juvenile limpets growing on the pygnogonids may be restricted in terms of lateral growth by the narrow form of the pygnogonid legs, resulting in an elongated footprint. After leaving the pycnogonid and continuing to grow on different substrata, e.g., basalts or chimneys, the footprint of the limpet may be somewhat fixed in shape during adult growth. Why the young limpets were commonly observed growing on the limbs of pygnogonids at the Kemp Caldera but not at E2 or E9 is a question we cannot answer presently. It may be that *L. concentricus* n. sp. was preferentially epizoic on *Kiwa tyleri* and *N. scotiaensis* or on basalts substrata at E2 and E9 (Marsh et al., 2012; Rogers et al., 2012). In the Kemp Caldera, the absence of *Kiwa* and the rarity of *Neolepas* barnacles, as well as differences in substratum, such as the presence of elemental sulphur on and near the chimneys at the Kemp Caldera, possibly left the pycnogonids as the optimal surfaces for juveniles to inhabit. Although there is some genetic separation between the ESR and Kemp Caldera populations of *L. concentricus* n. sp. (**Figure 6**) which may have some contribution to the morphological differences seen between the two populations, this is unlikely to be the primary cause as the degree of genetic separation appears very small (Roterman et al., 2016).

The shell profile (i.e., flat vs. tall domed morphology) of limpet-formed gastropods have been both observed (e.g., Vat, 2000; Warén and Bouchet, 2009) and experimentally shown (e.g., Lindberg and Pearse, 1990) to be strongly influenced by substratum morphology and type. Limpet-form has been evolved over 50 times in gastropods (Vermeij, 2016), and the apparent presence of similar substrate-dependent shell morphology plasticity on *Lepetedrilus concentricus* n. sp. reinforces the idea that such plasticity is not phylogenetically constrained but an inherent feature of being limpet-formed. In fact, *L. concentricus* n. sp. is not be the first gastropod known to exhibit phenotypic plasticity when growing on narrow substrates such as legs of pygnogonids, as the Antarctic gastropods *Capulus subcompressus* and *Dickdellia labioflecta* were reported to have adaptive morphology when growing on calcareous tubes of the serpulid polychaete *Serpula narconensis* (Schiaparelli et al., 2000, 2008) and in the case of *D. labioflecta* also on different pycnogonid species (Sirenko, 2000).

Environmental condition is another factor known to influence the phenotypic plasticity in animals (Pigliucci, 2005). In hydrothermal vent ecosystems, abiotic factors such as sulphide concentration, temperature and oxygen are known to affect the metabolic rates and therefore growth-linked morphology in aerobic organisms living there (e.g., Lutz et al., 1985; Girguis and Childress, 2006; Bergquist et al., 2007; Hourdez and Lallier, 2007; Tunnicliffe et al., 2014). Differences in these abiotic factors between and within the ESR vents and the Kemp Caldera (Rogers et al., 2012; Cole et al., 2014; Hawkes et al., 2014; James et al., 2014) has been suggested to be a key factor behind the high morphological plasticity in ESR and Kemp Caldera species. The eolepadid stalked barnacle *N. scotiaensis* which is also known from the three sites inhabited by *L. concentricus* n. sp., also exhibit an extraordinary range of morphological variation (Buckeridge et al., 2013). The "gracile" phenotype of *N. scotiaensis* occurred at sites of active diffuse venting (5–19°C), while the robust phenotype was found at sites with lower venting activity. Specimens of *L. concentricus* n. sp. were collected from the same localities as *N. scotiaensis* at E2 and E9, but phenotypic differences in shell morphology were not apparent between sites of low and active venting unlike the barnacles. Therefore, it is most likely that the morphological variations seen in *L. concentricus* n. sp. is due to a different reason than *N. scotiaensis*, with the aforementioned substrate type being the most likely factor.

Nevertheless, the vent fluids at the Kemp Caldera had a very high concentration of H_2S ($\sim$ 200 mM) and HF (1000 μM),

and probably other gases such as SO_2 and HCl, as a result of its location on the island back-arc system and the input of magmatically sourced acid volatiles (Cole et al., 2014). This is likely to result in a more acidic and corrosive environment than at E2 and E9, which are hosted in a more typical, mid-ocean ridge setting. These environmental differences may explain higher levels of corrosion of the prismatic shell layers of *L. concentricus* n. sp. seen at the Kemp Caldera (**Figures 3C,D**).

The length-frequency distributions of *L. concentricus* n. sp. at E9 and in the Kemp Caldera were positively skewed and numerically dominated by the smaller individuals. At E2 there were more large individuals with shell lengths of ∼9.0 mm. It was notable that at both ESR sites no young limpets with shell sizes <2.0 mm were collected, while the mesh size used on the suction sampler was 1.0 mm and at Kemp individuals as small as 1.0 mm in length were found. The paucity of small specimens is in agreement with Bates (2008) noting that specimens <1.0 mm shell length are difficult to collect by suction sampler. Similar size-frequency distributions with a positive skew toward smaller sizes have been reported several times in the literature for *Lepetodrilus*, for example *L. fucensis* (Bates, 2008; Kelly and Metaxas, 2008) and *L. tevianus* (Bayer et al., 2011). The size-frequency distribution of *L. elevatus* has also been reported to significantly differ between different vent sites, although the distributions were polymodal (Sadosky et al., 2002). It has also been suggested from that the physico-chemical environment of the immediate habitat has a significant impact on the population structure and reproductive biology of *L. elevatus* from the 13°N field of EPR, where small, immature individuals dominated more active and toxic habitats, inferring that juveniles may have a higher tolerance of unfavourable environmental conditions than adults (Matabos et al., 2008). On the other hand, Bates (2007) found that *L. fucensis* juveniles were common at vent periphery but rarer near highly active vent orifices. Taken together, these evidences suggest that it is common for *Lepetodrilus* species to have different tolerances to environmental stress at different size classes, but the effect may vary among different species. In the case of *L. concentricus* n. sp., the significantly more toxic and acidic conditions at Kemp compared to the other two localities mean that the dominance of smaller sized individuals there may partly be due to a similar scenario at *L. elevatus* from the 13°N field of EPR (Matabos et al., 2008) where juveniles appeared to be more tolerant to toxic, stressful environment. However, this does not explain why smaller individuals were also more dominant at E9 compared to E2, and incomplete size sampling cannot be ruled out.

Biotic interactions like predation might also have an influence on the size frequency distributions. At EPR, Sancho et al. (2005) studying the stomach contents of the vent-endemic, predatory eelpout *Thermarces cerberus* discovered that lepetodrillid gastropods were significant prey items with limpet from 0.9 to 11.9 mm shell length found to be digested. At the ESR vent sites E2 and E9 no fish were observed present near the chimneys or in the diffuse flow areas (K. Linse, personal observation). In the Kemp Caldera, fish were present in near-bottom, non-venting areas, e.g., two different macrouid species (rattails), a muraenolepid and the paralepidid *Notolepis annulata,* but rarely in venting areas, while fish observed there were seen dropping and dying if swimming too close to the seafloor (K. Linse, personal observation).

Given lepetodrilids are thought to reproduce continually and to produce free-swimming larvae with a planktonic dispersal stage, their populations are thought to exhibit no size cohorts and to be successful colonisers (Kelly et al., 2007; Tyler et al., 2008; Kelly and Metaxas, 2010; Bayer et al., 2011). If this is the case with *L. concentricus* n. sp., then the absence of young, small-sized (<2 mm) specimens might either be a sampling artefact of using the ROV suction sampler for collection, or alternatively, may indicate that there have been no recent colonisation events. The absence of individuals smaller than 3.8 mm in length at E2, as well as the apparent binomial distribution of sizes may therefore be indicative of episodes of unreliable local recruitment or of incomplete size sampling.

The observed male-biassed sex ratio in *L. concentricus* n. sp. appears to contrast with observations of equal sex representation in *L. fucensis* from the Juan de Fuca Ridge in the northeast Pacific (Bates, 2008). Bayer et al. (2011) analysed the sex in individual of *L. tevnianus* from settlement plates at 9°50′N ESR and in the determinable specimens, more females were observed than males. Kelly and Metaxas (2008) also discovered sex-biassed habitat partitioning in *L. fucensis* with juveniles and males preferring the periphery while females occurred in higher proportions in high fluid flow areas. The current data from this study do not indicate distinct sex-based habitat partitioning as seen with *L. fucensis* (Kelly and Metaxas, 2008), but the largest sex-determined specimens of *L. concentricus* n. sp. at E2 were males from the flanks of active chimneys and this suggests a habitat influence. Nevertheless, the possibility that the apparent bias in sex ratio reported here may be an artefact of incomplete sampling around the vents and the vicinity cannot be excluded entirely.

CONCLUSION

We reported *Lepetodrilus concentricus* n. sp. from three hydrothermal vent fields on the ESR and South Sandwich Arc, with phylogenetic analysis using the mitochondrial COI gene confirming a single MOTU across populations from all three vents. The shell profile of *L. concentricus* n. sp. is remarkably plastic and variable, which we infer to be most likely due to responses to differences in substrate type and morphology. Based on the examined specimens, size and sex-based habitat partitioning in *L. concentricus* n. sp. appears different to those reported in *L. fucensis* and *L. tevnianus* (Bates, 2008; Bayer et al., 2011). The size frequency analysis examining the population structure in *L. concentricus* is consistent with continuous reproduction. Further, in-depth ecological studies at similar hydrothermal systems are required to examine the applicability of using such rates on species found inhabiting different hydrothermal systems.

DATA AVAILABILITY

The datasets generated for this study are available in the Genbank, KP757039-KP757103.

ETHICS STATEMENT

Study species were gastropod molluscs preserved in either formalin or ethanol, no experiments with live animals were undertaken for the present study. The fieldwork in the East Scotia Sea during JC42 was undertaken under the permit S3-3/2009 issued by the Foreign and Commonwealth Office, London to section 3 of the Antarctic Act 1994.

AUTHOR CONTRIBUTIONS

KL conceived and designed the study, collected and analysed the morphological data, and carried out all microscopical experiments. KL and CC interpreted the morphological data. KL and CNR collected the genetics data, took part in the collection of samples and data used in this study, and drafted the original manuscript which was critically revised and improved by CC. CNR analysed and interpreted the genetics data. All authors prepared the figures and tables and gave final approval for submission and publication.

FUNDING

This research and the RRS *James Cook* expedition JC42 were supported by the ChEsSo (Chemosynthetic Ecosystems of the Southern Ocean) programme led by Paul Tyler, funded by a UK NERC Consortium Grant (NE/DO1249X/1).

ACKNOWLEDGMENTS

We are extremely grateful to Paul Tyler as the principal investigator of the ChEsSo research programme, and for enabling us to be part of the team. We thank Alex Rogers as the PSO of the RRS *James Cook* cruise JC42, the master and crew of the RRS *James Cook*, and the staff of the UK National Marine Facilities at the NOC, especially the pilots and technical teams of the ROV *Isis*, for their tremendous logistic and shipboard support during the fieldwork in the Southern Ocean. We are also grateful to Veerle Huvenne for the map used herein, Elaine Fitzcharles for PCR amplifications, and Pete Bucktrout for the macrophotographs. All authors are part of the ChEsSO research programme.

REFERENCES

Amon, D. J., Glover, A. G., Copley, J. T., Wiklund, H., and Linse, K. (2013). New insights into the fate of cetacean carcasses: the discovery of a natural whale fall in the Antarctic deep sea. *Deep-Sea Res. Part II Top. Stud. Oceanogr.* 92, 87–96. doi: 10.1016/j.dsr2.2013.01.028

Arango, C., and Linse, K. (2015). New *Sericosura* (*Pycnogonida*: *Ammotheidae*) from deep-sea hydrothermal vents in the Southern Ocean. *Zootaxa* 3995, 037–050. doi: 10.11646/zootaxa.3995.1.5

Bandelt, H.-J., Forster, P., and Röhl, A. (1999). Median-joining networks for inferring intraspecific phylogenies. *Mol. Biol. Evol.* 16, 37–48. doi: 10.1093/oxfordjournals.molbev.a026036

Barker, P. F., and Lawver, L. A. (1988). South American-Antarctic plate motion over the past 50 Myr, and the evolution of the South American-Antarctic ridge. *Geophys. J. Int.* 94, 377–386. doi: 10.1111/j.1365-246X.1988.tb02261.x

Bates, A. E. (2007). Feeding strategy, morphological specialisation and presence of bacterial episymbionts in lepetodrilid gastropods from hydrothermal vents. *Mar. Ecol. Progr. Ser.* 347, 87–99. doi: 10.3354/meps07020

Bates, A. E. (2008). Size- and sex-based habitat partitioning by *Lepetodrilus fucensis* near hydrothermal vents on the Juan de Fuca Ridge, Northeast Pacific. *Can. J. Fish. Aquat. Sci.* 65, 2332–2341. doi: 10.1139/f08-139

Bayer, S. R., Mullineaux, L. S., Waller, R. G., and Solow, A. R. (2011). Reproductive traits of pioneer gastropod species colonizing deep-sea hydrothermal vents after an eruption. *Mar. Biol.* 158, 181–192. doi: 10.1007/s00227-010-1550-1

Bergquist, D. C., Eckner, J. T., Urcuyo, I. A., Cordes, E. E., Hourdez, S., Macko, S. A., et al. (2007). Using stable isotopes and quantitative community characteristics to determine a local hydrothermal vent food web. *Mar. Ecol. Progr. Ser.* 330, 49–65. doi: 10.3354/meps330049

Buckeridge, J. S., Linse, K., and Jackson, J. A. (2013). *Vulcanolepas scotiaensis* sp. nov., a new deep-sea scalpelliform barnacle (Eolepadidae: Neolepadinae) from hydrothermal vents in the Scotia Sea, Antarctica. Zootaxa 3745, 551–568. doi: 10.11646/zootaxa.3745.5.4

Chen, C., Linse, K., Roterman, C. N., Copley, J. T., and Rogers, A. D. (2015). A new genus of large hydrothermal vent-endemic gastropod (Neomphalina: Peltospiridae) with two new species showing evidence of recent demographic expansion. *Zool. J. Linn. Soc.* 175, 319–335. doi: 10.1111/zoj.12279

Cole, C. S., James, R. H., Connelly, D. P., and Hathorne, E. C. (2014). Rare earth elements as indicators of hydrothermal processes within the East Scotia subduction zone system. *Geochem. Cosmochem. Acta* 140, 20–38. doi: 10.1016/j.gca.2014.05.018

Copley, J. T., Marsh, L., Glover, A. G., Huhnerbach, V., Nye, V. E., Reid, W. D. K., et al. (2016). Ecology and biogeography of megafauna and macrofauna at the first known deep-sea hydrothermal vents on the ultraslow-spreading Southwest Indian Ridge. *Sci. Rep.* 6:39158. doi: 10.1038/srep39158

Cortese, G., and Gersonde, R. (2008). Plio/Pleistocene changes in the main biogenic silica carrier in the Southern Ocean, Atlantic Sector. *Mar. Geol.* 252, 100–110. doi: 10.1016/j.margeo.2008.03.015

Drummond, A., Ashton, B., Cheung, M., Heled, J., Kearse, M., and Moir, R. (2010). *Geneious v5.5*. Available at: http://www.geneious.com (accessed March 12, 2012).

Felsenstein, J. (2002). *{PHYLIP}(Phylogeny Inference Package) Version 3.6 a3*.

Folmer, O., Black, M., Hoeh, W., Lutz, R., and Vrijenhoek, R. (1994). DNA primers for amplification of mitochondrial cytochrome c oxidase subunit I from diverse metazoan invertebrates. *Mol. Mar. Biol. Biotechnol.* 3:294.

Gaudron, S. M., Marqué, L., Thiébaut, E., Riera, P., Duperron, S., and Zbinden, M. (2015). How are microbial and detrital sources partitioned among and within gastropods species at East Pacific Rise hydrothermal vents? *Mar. Ecol.* 36, 18–34. doi: 10.1111/maec.12260

Girguis, P. R., and Childress, J. J. (2006). Metabolite uptake, stoichiometry and chemoautotrophic function of the hydrothermal vent tubeworm *Riftia pachyptila*: responses to environmental variations in substrate concentrations and temperature. *J. Exp. Biol.* 209, 3516–3528. doi: 10.1242/jeb.02404

Guindon, S., Dufayard, J.-F., Lefort, V., Anisimova, M., Hordijk, W., and Gascuel, O. (2010). New algorithms and methods to estimate maximum-likelihood phylogenies: assessing the performance of PhyML 3.0. *Syst. Biol.* 59, 307–321. doi: 10.1093/sysbio/syq010

Hawkes, J. A., Connelly, D. P., Rijkenberg, M. J. A., and Achterberg, E. P. (2014). The importance of shallow hydrothermal island arc systems in ocean biogeochemistry. *Geophys. Res. Lett.* 41, 942–947. doi: 10.1002/2013GL058817

Herrera, S., Watanabe, H., and Shank, T. M. (2015). Evolutionary and biogeographical patterns of barnacles from deep-sea hydrothermal vents. *Mol. Ecol.* 24, 673–689. doi: 10.1111/mec.13054

Hey, R. N., and Wilson, D. S. (1982). Propagating rift explanation for the tectonic evolution of the northeast Pacific—the pseudomovie. *Earth Planet. Sci. Lett.* 58, 167–184. doi: 10.1016/0012-821X(82)90192-3

Ho, S. Y. W., Lanfear, R., Bromham, L., Phillips, M. J., Soubrier, J., Rodrigo, A. G., et al. (2011). Time-dependent rates of molecular evolution. *Mol. Ecol.* 20, 3087–3101. doi: 10.1111/j.1365-294X.2011.05178.x

Ho, S. Y. W., and Phillips, M. J. (2009). Accounting for calibration uncertainty in phylogenetic estimation of evolutionary divergence times. *Systemat. Biol.* 58, 367–380. doi: 10.1093/sysbio/syp035

Hourdez, S., and Lallier, F. H. (2007). Adaptations to hypoxia in hydrothermal vent and cold-seep invertebrates. *Rev. Environ. Sci. Biotech.* 6, 143–159. doi: 10.1007/s00441-009-0811-0

James, R. H., Green, D. R. H., Stock, M. J., Alker, B. J., Banerjee, N. R., Cole, C., et al. (2014). Composition of hydrothermal fluids and mineralogy of associated chimney material on the East Scotia Ridge back-arc spreading centre. *Geochim. Cosmochim. Acta* 139, 47–71. doi: 10.1016/j.gca.2014.04.024

Johnson, S. B., Warén, A., and Vrijenhoek, R. C. (2008). DNA barcoding of *Lepetodrilus* limpets reveals cryptic species". *J. Shellfish Res.* 27, 43–51. doi: 10.2983/0730-8000(2008)27%5B43:dbollr%5D2.0.co;2

Johnson, S. B., Young, C. R., Jones, W. J., Warén, A., and Vrijenhoek, R. C. (2006). Migration, isolation, and speciation of hydrothermal vent limpets (Gastropoda; Lepetodrillidae) across the blanco transform fault. *Biol. Bull.* 210, 140–157. doi: 10.2307/4134603

Kano, Y. (2008). Vetigastropod phylogeny and a new concept of *Seguenzioidea*: independent evolution of copulatory organs in the deep-sea habitat. *Zool. Scrip.* 37, 1–21. doi: 10.1111/j.1463-6409.2007.00316.x

Kelly, N., and Metaxas, A. (2008). Population structure of two deep-sea hydrothermal vent gastropods from the Juan de Fuca Ridge, NE Pacific. *Mar. Biol.* 153, 457–471. doi: 10.1007/s00227-007-0828-4

Kelly, N., and Metaxas, A. (2010). Understanding population dynamics of a numerically dominant species at hydrothermal vents: a matrix modelling approach. *Mar. Ecol. Progr. Ser.* 403, 113–128. doi: 10.3354/meps08442

Kelly, N., Metaxas, A., and Butterfield, D. (2007). Spatial and temporal patterns of colonization by deep-sea hydrothermal vent invertebrates on the Juan de Fuca Ridge, NE Pacific. *Aquat. Biol.* 1, 1–16. doi: 10.3354/ab00001

Kumar, S., Stecher, G., and Tamura, K. (2016). MEGA7: molecular evolutionary genetics analysis version 7.0 for bigger datasets. *Mol. Biol. Evol.* 33, 1870–1874. doi: 10.1093/molbev/msw054

Lanfear, R., Frandsen, P. B., Wright, A. M., Senfeld, T., and Calcott, B. (2016). PartitionFinder 2: new methods for selecting partitioned models of evolution for molecular and morphological phylogenetic analyses. *Mol. Biol. Evol.* 34, 772–773. doi: 10.1093/molbev/msw260

Larter, R. D., Vanneste, L. E., Morris, P., and Smythe, D. K. (2003). Structure and tectonic evolution of the South Sandwich arc. *Geol. Soc.* 219:255. doi: 10.1144/gsl.sp.2003.219.01.13

Layton, K. K. S., Martel, A. L., and Hebert, P. D. N. (2014). Patterns of DNA barcode variation in Canadian marine molluscs. *PLoS One* 9:e95003. doi: 10.1371/journal.pone.0095003

Leese, F., Brand, P., Kuzmin, A., Mayer, C., Agrawal, S., Dambach, J., et al. (2012). Exploring pandora's box: potential and pitfalls of low coverage genome surveys for evolutionary biology. *PLoS One* 7:e49202. doi: 10.1371/journal.pone.0049202

Ligi, M., Bonatti, E., Bortoluzzi, G., Carrara, G., Fabretti, P., Gilod, D., et al. (1999). Bouvet triple junction in the South Atlantic: geology and evolution. *J. Geophys. Res.* 104, 29365–29385. doi: 10.1029/1999JB900192

Lindberg, D. R., and Pearse, J. S. (1990). Experimental manipulation of shell colour and morphology of the limpets *Lottia asmi* (Middendorff) and *Lottia digitalis* (Rathke) (Mollusca:Patellogastropoda). *J. Exp. Mar. Biol. Eecol.* 140, 173–185. doi: 10.1016/0022-0981(90)90125-v

Littlewood, D. T. J. (1994). Molecular phylogenetics of cupped oysters based on partial 28S rRNA gene sequences. *Mol. Phylogenet. Evol.* 3, 221–229. doi: 10.1006/mpev.1994.1024

Lutz, R. A., Fritz, L. W., and Rhoads, D. C. (1985). Molluscan growth at deep-sea hydrothermal vents. *Bull. Biol. Soc.* 6, 199–210.

Marsh, L., Copley, J. T., Huvenne, V. A. I., Linse, K., Reid, W. D. K., Rogers, A. D., et al. (2012). Microdistribution of faunal assemblages at deep-sea hydrothermal vents in the Southern Ocean. *PLoS One* 7:e48348. doi: 10.1371/journal.pone.0048348

Matabos, M., and Jollivet, D. (2019). Revisiting the *Lepetodrilus elevatus* species complex (Vetigastropoda: Lepetodrilidae), using samples from the Galápagos and Guaymas hydrothermal vent systems. *J. Mollusc. Stud.* 85, 154–165. doi: 10.1093/mollus/eyy061

Matabos, M., Le Bris, N., Pendlebury, S., and Thiébaut, E. (2008). Role of physico-chemical environment on gastropod assemblages at hydrothermal vents on the East Pacific Rise (13°N/EPR). *J. Mar. Biol. Assoc. U.K.* 88, 995–1008. doi: 10.1017/s002531540800163x

McLean, J. H. (1988). New archaeogastropod limpets from hydrothermal vents; superfamily lepetodrilacea I. systematic descriptions. *Philos. Trans. R. Soc. B* 319, 1–32. doi: 10.1098/rstb.1988.0031

Medlin, L. K., Elwood, H. J., Stickel, S., and Sogin, M. L. (1988). The characterization of enzymatically amplified eukaryotic 16S-like rRNA-coding regions. *Gene* 71, 491–499. doi: 10.1016/0378-1119(88)90066-2

MolluscaBase. (2019). *MolluscaBase. Lepetodrilus McLean, 1988. World Register of Marine Species*. Available at: http://www.marinespecies.org/aphia.php?p=taxdetails&id=180907 (accessed April 01, 2019).

Naar, D. F., and Hey, R. N. (1991). Tectonic evolution of the Easter microplate. *J. Geophys. Res.* 96, 7961–7993.

Nakamura, M., Watanabe, H., Sasaki, T., Ishibashi, J., Fujikura, K., and Mitarai, S. (2014). Life history traits of *Lepetodriluls nux* in the Okinawa Trough, based upon gametogenesis, shell size, and genetic variability. *Mar. Ecol. Progr. Ser.* 505, 119–130. doi: 10.3354/meps10779

Nguyen, L.-T., Schmidt, H. A., von Haeseler, A., and Minh, B. Q. (2015). IQ-TREE: a fast and effective stochastic algorithm for estimating maximum-likelihood phylogenies. *Mol. Biol. Evol.* 32, 268–274. doi: 10.1093/molbev/msu300

Okutani, T., Fujikura, K., and Sasaki, T. (1993). New taxa and new distribution records of deep-sea gastropods collected from or near the chemosynthetic communities in the Japanese waters. *Bull. Natl. Sci. Mus.* 19, 123–143.

Pigliucci, M. (2005). Evolution of phenotypic plasticity: where are we going now? *Trends Ecol. Evol.* 20, 481–486. doi: 10.1016/j.tree.2005.06.001

Puillandre, N., Lambert, A., Brouillet, S., and Achaz, G. (2012). ABGD, automatic barcode gap discovery for primary species delimitation. *Mol. Ecol.* 21, 1864–1877. doi: 10.1111/j.1365-294X.2011.05239.x

Rambaut, A., Drummond, A. J., Xie, D., Baele, G., and Suchard, M. A. (2018). Posterior Summarization in bayesian phylogenetics using tracer 1.7. *Systemat. Biol.* 67, 901–904. doi: 10.1093/sysbio/syy032

Reid, W. D. K., Sweeting, C. J., Wigham, B. D., Zwirglmaier, K., Hawkes, J. A., McGill, R. A. R., et al. (2013). Spatial differences in East Scotia ridge hydrothermal vent food webs: influences of chemistry, microbiology and predation on trophodynamics. *PLoS One* 8:e065553. doi: 10.1371/journal.pone.0065553

Rogers, A. D., and Linse, K. (2014). "Chemosynthetic communities," in *Proceedings of the CAML/ SCAR MarBIN Biogeographic Atlas of the Southern Ocean Strategic Science in Antarctica. A joint Australian and New Zealand conference*, eds C. De Broyer, et al. Hobart.

Rogers, A. D., Tyler, P. A., Connelly, D. P., Copley, J. T., James, R., Larter, R. D., et al. (2012). The discovery of new deep-sea hydrothermal vent communities in the Southern Ocean and implications for biogeography. *PLoS Biol.* 10:e1001234. doi: 10.1371/journal.pbio.1001234

Ronquist, F., and Huelsenbeck, J. P. (2003). MrBayes 3: Bayesian phylogenetic inference under mixed models. *Bioinformatics* 19, 1572–1574. doi: 10.1093/bioinformatics/btg180

Roterman, C. B., Copley, J. T., Linse, K., Tyler, P. A., and Rogers, A. D. (2016). Connectivity in the cold: the comparative population genetics of vent-endemic fauna in the Scotia Sea. Southern Ocean. *Mol. Ecol.* 25, 1073–1088. doi: 10.1111/mec.13541

Roterman, C. N., Copley, J. T., Linse, K., Tyler, P. A., and Rogers, A. D. (2013a). Development of polymorphic microsatellite loci for three species of vent-endemic megafauna from deep-sea hydrothermal vents in the Scotia Sea, Southern Ocean. *Conserv. Genet. Res.* 5, 835–839. doi: 10.1007/s12686-01309921-9

Roterman, C. N., Copley, J. T., Linse, K., Tyler, P. A., and Rogers, A. D. (2013b). The biogeography of the yeti crabs (Kiwaidae) with notes on the phylogeny of the *Chirostyloidea* (Decapoda: Anomura). *Proc. R. Soc. B* 280:20130718. doi: 10.1098/rspb.2013.0718

Roterman, C. N., Lee, W.-K., Liu, X., Lin, R., Li, X., and Won, Y.-J. (2018). A new yeti crab phylogeny: vent origins with indications of regional extinction in the East Pacific. *PLos One* 13:e0194696. doi: 10.1371/journal.pone.0194696

Rusby, R. I., and Searle, R. C. (1995). A history of the Easter microplate, 5.25 Ma to present. *J. Geophys. Res.* 100, 12617–12640. doi: 10.1029/94jb02779

Sadosky, F., Thiebaut, E., Jollivet, D., and Shillito, B. (2002). Recruitment and population structure of the vetigastropod Lepetodrilus elevatus at 13°N hydothermal vent sites on East Pacific Rise. *Cahiers Biol. Mar.* 43, 399–402.

Salvini-Plawen, L. (1980). A reconsideration of systematic in the mollusca (phylogeny and higher classification). *Malacologia* 19, 249–278.

Sancho, G., Fisher, C. R., Mills, S., Micheli, F., Johnson, G. A., Lenihan, H. S., et al. (2005). Selective predation by the zoarcid fish *Thermarces cerberus* at hydrothermal vents. *Deep-Sea Res. I* 52, 837–844. doi: 10.1016/j.dsr.2004.12.002

Schiaparelli, S., Cattaneo-Vietti, R., and Chiatore, M. (2000). Adaptive morphology of *Capulus subcompressus* Pelseneer, 1903 (Gastropoda: Capulidae) from Terra Nova Bay, Ross Sea (Antarctica). *Polar Biol.* 23, 11–16. doi: 10.1007/s003000050002

Schiaparelli, S., Oliverio, M., Taviani, M., Griffiths, H. J., Loerz, A.-N., and Albertelli, G. (2008). Circumpolar distribution of the pycnogonid-ectoparasitic gastropod *Dickdellia labioflecta* (Dell, 1990) (Mollusca: Zerotulidae). *Antarct. Sci.* 20, 497–498. doi: 10.1017/s0954102008001302

Sirenko, B. I. (2000). Symbiosis of an Antarctic gastropod and pantopod. *Ruthenica* 10, 159–162.

Suchard, M. A., Lemey, P., Baele, G., Ayres, D. L., Drummond, A. J., and Rambaut, A. (2018). Bayesian phylogenetic and phylodynamic data integration using BEAST 1.10. *Virus Evol.* 4:170. doi: 10.1093/ve/vey016

Tamura, K., Battistuzzi, F. U., Billing-Ross, P., Murillo, O., Filipski, A., and Kumar, S. (2012). Estimating divergence times in large molecular phylogenies. *Proc. Natl. Acad. Sci. USA* 109, 19333–19338. doi: 10.1073/pnas.1213199109

Thatje, S., Marsh, L., Roterman, C. N., Mavrogordato, M. N., and Linse, K. (2015). Adaptations to hydrothermal vent life in *Kiwa tyleri*, a new species of yeti crab from the last Scotia Ridge, Antarctica. *PLoS One* 10:e0127621. doi: 10.1371/journal.pone.0127621

Tunnicliffe, V., St. Germain, C., and Hilario, A. (2014). Phenotypic variation and fitness in a metapopulation of tubeworms (*Ridgeia piscaesae* Jones) at hydrothermal vents. *PLoS One* 9:e110578. doi: 10.1371/journal.pone.0110578

Tyler, P. A., Pendlebury, S., Mills, S. W., Mullineaux, L., Eckelbarger, K. E., Baker, M., et al. (2008). Reproduction of gastropods from vents on the East Pacific Rise and the mid-Atlantic Ridge. *J. Shellfish Res.* 27, 107–118. doi: 10.2983/0730-8000(2008)27%5B107:rogfvo%5D2.0.co;2

Tyler, P. A., and Young, C. M. (2003). Dispersal at hydrothermal vents: a summary of recent progress. *Hydrobiologia* 503, 9–19. doi: 10.1023/b:hydr.0000008492.53394.6b

Vat, L. S. (2000). *The growth and reproduction of Patella granularis (Mollusca: Patellogastropoda) on the Southeast Coast of South Africa*. Ph.D. thesis, Rhodes University, Grahamstown, SA, 262.

Vérard, C., Flores, K., and Stampfli, G. (2012). Geodynamic reconstructions of the South America-Antarctica plate system. *J. Geodyn.* 53, 43–60. doi: 10.1016/j.jog.2011.07.007

Vermeij, G. J. (2016). The limpet form in gastropods: evolution, distribution, and implications for the comparative study of history. *Biol. J. Linn. Soc.* 120, 22–37

Vrijenhoek, R. C. (2013). On the instability and evolutionary age of deep-sea chemosynthetic communities. *Deep Sea Res. Part II Top. Stud. Oceanogr.* 92, 189–200. doi: 10.1016/j.dsr2.2012.12.004

Warén, A., and Bouchet, P. (2009). New gastropods from deep-sea hydrocarbon seeps off West Africa. *Deep-Sea Res. II Top. Stud. Oceanogr.* 56, 2326–2349. doi: 10.1016/j.dsr2.2009.04.013

Warén, A., Bouchet, P., and von Cosel, R. (2006). "*Lepetodrilus* McLean, 1988, "dimorphic limpets"," in *Handbook of Deep-Sea Hydrothermal Vent Fauna*, 2nd Edn, eds D. Desbruyères, M. Segonzac, and M. Bright (Linz: Biologiezentrum der Oberösterreichischen Landesmuseen).

Wilson, D. S., Hey, R. N., and Nishimura, C. (1984). Propagation as a mechanism of reorientation of the Juan de Fuca Ridge. *J. Geophys. Res. Solid Earth* 89, 9215–9225. doi: 10.1029/JB089iB11p09215

Conflict of Interest Statement: The authors declare that the research was conducted in the absence of any commercial or financial relationships that could be construed as a potential conflict of interest.